(12) INTERNATIONAL APPLICATION PUBLISHED UNDER THE PATENT COOPERATION TREATY (PCT)

(19) World Intellectual Property Organization
International Bureau

(43) International Publication Date
10 January 2013 (10.01.2013)

WIPO | PCT

(10) International Publication Number
WO 2013/006803 A2

(51) International Patent Classification:
H01L 31/0687 (2012.01)

(21) International Application Number:
PCT/US2012/045778

(22) International Filing Date:
6 July 2012 (06.07.2012)

(25) Filing Language: English

(26) Publication Language: English

(30) Priority Data:
61/505,014 6 July 2011 (06.07.2011) US

(72) Inventors; and

(71) Applicants : **FORREST, Stephen, R.** [US/US]; 336 Rock Creek Court, Ann Arbor, MI 48104 (US). **RENSHAW, Christopher, Kyle** [US/US]. **SLOOTHY, Michael** [US/US]; 1939 McIntrye Street, Ann Arbor, MI 48105 (US).

(74) Agent: **SWEET, Mark, D.**; Finnegan, Henderson, Farabow, Garrett & Dunner LLP, 901 New York Avenue, N.W., Washington, DC 20001 (US).

(81) Designated States *(unless otherwise indicated, for every kind of national protection available)*: AE, AG, AL, AM, AO, AT, AU, AZ, BA, BB, BG, BH, BR, BW, BY, BZ, CA, CH, CL, CN, CO, CR, CU, CZ, DE, DK, DM, DO, DZ, EC, EE, EG, ES, FI, GB, GD, GE, GH, GM, GT, HN, HR, HU, ID, IL, IN, IS, JP, KE, KG, KM, KN, KP, KR, KZ, LA, LC, LK, LR, LS, LT, LU, LY, MA, MD, ME, MG, MK, MN, MW, MX, MY, MZ, NA, NG, NI, NO, NZ, OM, PE, PG, PH, PL, PT, QA, RO, RS, RU, RW, SC, SD, SE, SG, SK, SL, SM, ST, SV, SY, TH, TJ, TM, TN, TR, TT, TZ, UA, UG, US, UZ, VC, VN, ZA, ZM, ZW.

(84) Designated States *(unless otherwise indicated, for every kind of regional protection available)*: ARIPO (BW, GH, GM, KE, LR, LS, MW, MZ, NA, RW, SD, SL, SZ, TZ, UG, ZM, ZW), Eurasian (AM, AZ, BY, KG, KZ, RU, TJ, TM), European (AL, AT, BE, BG, CH, CY, CZ, DE, DK, EE, ES, FI, FR, GB, GR, HR, HU, IE, IS, IT, LT, LU, LV, MC, MK, MT, NL, NO, PL, PT, RO, RS, SE, SI, SK, SM, TR), OAPI (BF, BJ, CF, CG, CI, CM, GA, GN, GQ, GW, ML, MR, NE, SN, TD, TG).

Published:

— *without international search report and to be republished upon receipt of that report (Rule 48.2(g))*

(54) Title: INTEGRATED SOLAR COLLECTORS USING EPITAXIAL LIFT OFF AND COLD WELD BONDED SEMICONDUCTOR SOLAR CELLS

(57) Abstract: There is disclosed ultrahigh-efficiency single- and multi-junction thin-film solar cells. This disclosure is also directed to a substrate-damage-free epitaxial lift-off ("ELO") process that employs adhesive-free, reliable and lightweight cold-weld bonding to a substrate, such as bonding to plastic or metal foils shaped into compound parabolic metal foil concentrators. By combining low-cost solar cell production and ultrahigh- efficiency of solar intensity-concentrated thin-film solar cells on foil substrates shaped into an integrated collector, as described herein, both lower cost of the module as well as significant cost reductions in the infrastructure is achieved.

WO 2013/006803 A2

INTEGRATED SOLAR COLLECTORS USING EPITAXIAL LIFT OFF AND COLD WELD BONDED SEMICONDUCTOR SOLAR CELLS

Cross-Reference to Related Application

[001] This application claims the benefit of U.S. Provisional Application No. 61/505,014, filed July 6, 2011, which is incorporated herein by reference in its entirety.

Joint Research Agreement

[002] The claimed invention was made by, on behalf of, and/or in connection with one or more of the following parties to a joint university-corporation research agreement: University of Michigan and Global Photonic Energy Corporation. The agreement was in effect on and before the date the invention was made, and the claimed invention was made as a result of activities undertaken within the scope of the agreement.

[003] This disclosure is directed to a ultrahigh-efficiency single- and multi-junction thin-film solar cells. This disclosure is also directed to a substrate-damage-free epitaxial lift-off ("ELO") process that employs adhesive-free, reliable and lightweight cold-weld bonding to a substrate, such as bonding to plastic or metal foils shaped into compound parabolic metal foil concentrators.

[004] Optoelectronic devices rely on the optical and electronic properties of materials to either produce or detect electromagnetic radiation electronically or to generate electricity from ambient electromagnetic radiation.

[005] Photosensitive optoelectronic devices convert electromagnetic radiation into electricity. Solar cells, also called photovoltaic (PV) devices, are a type of photosensitive optoelectronic device that is specifically used to generate electrical

power. PV devices, which may generate electrical energy from light sources other than sunlight, can be used to drive power consuming loads to provide, for example, lighting, heating, or to power electronic circuitry or devices such as calculators, radios, computers or remote monitoring or communications equipment. These power generation applications also often involve the charging of batteries or other energy storage devices so that operation may continue when direct illumination from the sun or other light sources is not available, or to balance the power output of the PV device with a specific application's requirements. As used herein the term "resistive load" refers to any power consuming or storing circuit, device, equipment or system.

[006] Another type of photosensitive optoelectronic device is a photoconductor cell. In this function, signal detection circuitry monitors the resistance of the device to detect changes due to the absorption of light.

[007] Another type of photosensitive optoelectronic device is a photodetector. In operation a photodetector is used in conjunction with a current detecting circuit which measures the current generated when the photodetector is exposed to electromagnetic radiation and may have an applied bias voltage. A detecting circuit as described herein is capable of providing a bias voltage to a photodetector and measuring the electronic response of the photodetector to electromagnetic radiation.

[008] These three classes of photosensitive optoelectronic devices may be characterized according to whether a rectifying junction as defined below is present and also according to whether the device is operated with an external applied voltage, also known as a bias or bias voltage. A photoconductor cell does not have a rectifying junction and is normally operated with a bias. A PV device has at least one rectifying

junction and is operated with no bias. A photodetector has at least one rectifying junction and is usually but not always operated with a bias. As a general rule, a photovoltaic cell provides power to a circuit, device or equipment, but does not provide a signal or current to control detection circuitry, or the output of information from the detection circuitry. In contrast, a photodetector or photoconductor provides a signal or current to control detection circuitry, or the output of information from the detection circuitry but does not provide power to the circuitry, device or equipment.

[009] Traditionally, photosensitive optoelectronic devices have been constructed of a number of inorganic semiconductors, *e.g.*, crystalline, polycrystalline and amorphous silicon, gallium arsenide, cadmium telluride and others. Herein the term "semiconductor" denotes materials which can conduct electricity when charge carriers are induced by thermal or electromagnetic excitation. The term "photoconductive" generally relates to the process in which electromagnetic radiant energy is absorbed and thereby converted to excitation energy of electric charge carriers so that the carriers can conduct, *i.e.*, transport, electric charge in a material. The terms "photoconductor" and "photoconductive material" are used herein to refer to semiconductor materials which are chosen for their property of absorbing electromagnetic radiation to generate electric charge carriers.

[010] PV devices may be characterized by the efficiency with which they can convert incident solar power to useful electric power. Devices utilizing crystalline or amorphous silicon dominate commercial applications, and some have achieved efficiencies of 23% or greater. However, efficient crystalline-based devices, especially of large surface area, are difficult and expensive to produce due to the problems

inherent in producing large crystals without significant efficiency-degrading defects. On the other hand, high efficiency amorphous silicon devices still suffer from problems with stability. Present commercially available amorphous silicon cells have stabilized efficiencies between 4 and 8%. More recent efforts have focused on the use of organic photovoltaic cells to achieve acceptable photovoltaic conversion efficiencies with economical production costs.

[011] PV devices may be optimized for maximum electrical power generation under standard illumination conditions (i.e., Standard Test Conditions which are 1000 W/m2, AM1.5 spectral illumination), for the maximum product of photocurrent times photovoltage. The power conversion efficiency of such a cell under standard illumination conditions depends on the following three parameters: (1) the current under zero bias, i.e., the short-circuit current I_{SC}, in Amperes (2) the photovoltage under open circuit conditions, i.e., the open circuit voltage V_{OC}, in Volts and (3) the fill factor, *ff*.

[012] PV devices produce a photo-generated current when they are connected across a load and are irradiated by light. When irradiated under infinite load, a PV device generates its maximum possible voltage, V open-circuit, or V_{OC}. When irradiated with its electrical contacts shorted, a PV device generates its maximum possible current, I short-circuit, or I_{SC}. When actually used to generate power, a PV device is connected to a finite resistive load and the power output is given by the product of the current and voltage, $I \times V$. The maximum total power generated by a PV device is inherently incapable of exceeding the product, $I_{SC} \times V_{OC}$. When the load value is optimized for maximum power extraction, the current and voltage have the values, I_{max} and V_{max}, respectively.

[013] A figure of merit for PV devices is the fill factor, *ff*, defined as:

$$ff = \{ I_{max} V_{max} \}/\{ I_{SC} V_{OC} \} \qquad (1)$$

where *ff* is always less than 1, as I_{SC} and V_{OC} are never obtained simultaneously in actual use. Nonetheless, as *ff* approaches 1, the device has less series or internal resistance and thus delivers a greater percentage of the product of I_{SC} and V_{OC} to the load under optimal conditions. Where P_{inc} is the power incident on a device, the power efficiency of the device, γ_P, may be calculated by:

$$\gamma_P = ff * (I_{SC} * V_{OC}) / P_{inc}$$

[014] When electromagnetic radiation of an appropriate energy is incident upon a semiconductive organic material, for example, an organic molecular crystal (OMC) material, or a polymer, a photon can be absorbed to produce an excited molecular state. This is represented symbolically as $S_0 + hv \Psi S_0^*$. Here S_0 and S_0^* denote ground and excited molecular states, respectively. This energy absorption is associated with the promotion of an electron from a bound state in the HOMO energy level, which may be a B-bond, to the LUMO energy level, which may be a B*-bond, or equivalently, the promotion of a hole from the LUMO energy level to the HOMO energy level. In organic thin-film photoconductors, the generated molecular state is generally believed to be an exciton, i.e., an electron-hole pair in a bound state which is transported as a quasi-particle. The excitons can have an appreciable life-time before geminate recombination, which refers to the process of the original electron and hole recombining with each other, as opposed to recombination with holes or electrons from other pairs. To produce a photocurrent the electron-hole pair becomes separated, typically at a donor-acceptor interface between two dissimilar contacting organic thin

films. If the charges do not separate, they can recombine in a geminant recombination process, also known as quenching, either radiatively, by the emission of light of a lower energy than the incident light, or non-radiatively, by the production of heat. Either of these outcomes is undesirable in a photosensitive optoelectronic device.

[015] Electric fields or inhomogeneities at a contact may cause an exciton to quench rather than dissociate at the donor-acceptor interface, resulting in no net contribution to the current. Therefore, it is desirable to keep photogenerated excitons away from the contacts. This has the effect of limiting the diffusion of excitons to the region near the junction so that the associated electric field has an increased opportunity to separate charge carriers liberated by the dissociation of the excitons near the junction.

[016] To produce internally generated electric fields which occupy a substantial volume, the usual method is to juxtapose two layers of material with appropriately selected conductive properties, especially with respect to their distribution of molecular quantum energy states. The interface of these two materials is called a photovoltaic heterojunction. In traditional semiconductor theory, materials for forming PV heterojunctions have been denoted as generally being of either n or p type. Here n-type denotes that the majority carrier type is the electron. This could be viewed as the material having many electrons in relatively free energy states. The p-type denotes that the majority carrier type is the hole. Such material has many holes in relatively free energy states. The type of the background, i.e., not photo-generated, majority carrier concentration depends primarily on unintentional doping by defects or impurities. The type and concentration of impurities determine the value of the Fermi energy, or level,

within the gap between the highest occupied molecular orbital (HOMO) energy level and the lowest unoccupied molecular orbital (LUMO) energy level, called the HOMO-LUMO gap. The Fermi energy characterizes the statistical occupation of molecular quantum energy states denoted by the value of energy for which the probability of occupation is equal to ½. A Fermi energy near the LUMO energy level indicates that electrons are the predominant carrier. A Fermi energy near the HOMO energy level indicates that holes are the predominant carrier. Accordingly, the Fermi energy is a primary characterizing property of traditional semiconductors and the prototypical PV heterojunction has traditionally been the p-n interface.

[017] The term "rectifying" denotes, *inter alia*, that an interface has an asymmetric conduction characteristic, i.e., the interface supports electronic charge transport preferably in one direction. Rectification is associated normally with a built-in electric field which occurs at the heterojunction between appropriately selected materials.

[018] As used herein, and as would be generally understood by one skilled in the art, a first "Highest Occupied Molecular Orbital" (HOMO) or "Lowest Unoccupied Molecular Orbital" (LUMO) energy level is "greater than" or "higher than" a second HOMO or LUMO energy level if the first energy level is closer to the vacuum energy level. Since ionization potentials (IP) are measured as a negative energy relative to a vacuum level, a higher HOMO energy level corresponds to an IP having a smaller absolute value (an IP that is less negative). Similarly, a higher LUMO energy level corresponds to an electron affinity (EA) having a smaller absolute value (an EA that is less negative). On a conventional energy level diagram, with the vacuum level at the

top, the LUMO energy level of a material is higher than the HOMO energy level of the same material. A "higher" HOMO or LUMO energy level appears closer to the top of such a diagram than a "lower" HOMO or LUMO energy level.

[019] In the context of organic materials, the terms "donor" and "acceptor" refer to the relative positions of the HOMO and LUMO energy levels of two contacting but different organic materials. This is in contrast to the use of these terms in the inorganic context, where "donor" and "acceptor" may refer to types of dopants that may be used to create inorganic n- and p- types layers, respectively. In the organic context, if the LUMO energy level of one material in contact with another is lower, then that material is an acceptor. Otherwise it is a donor. It is energetically favorable, in the absence of an external bias, for electrons at a donor-acceptor junction to move into the acceptor material, and for holes to move into the donor material.

[020] A significant property in organic semiconductors is carrier mobility. Mobility measures the ease with which a charge carrier can move through a conducting material in response to an electric field. In the context of organic photosensitive devices, a layer including a material that conducts preferentially by electrons due to a high electron mobility may be referred to as an electron transport layer, or ETL. A layer including a material that conducts preferentially by holes due to a high hole mobility may be referred to as a hole transport layer, or HTL. Preferably, but not necessarily, an acceptor material is an ETL and a donor material is a HTL.

[021] Conventional inorganic semiconductor PV cells employ a p-n junction to establish an internal field. Early organic thin film cell, such as reported by Tang, *Appl. Phys Lett.* **48**, 183 (1986), contain a heterojunction analogous to that employed in a

conventional inorganic PV cell. However, it is now recognized that in addition to the establishment of a p-n type junction, the energy level offset of the heterojunction also plays an important role.

[022] The energy level offset at the organic D-A heterojunction is believed to be important to the operation of organic PV devices due to the fundamental nature of the photogeneration process in organic materials. Upon optical excitation of an organic material, localized Frenkel or charge-transfer excitons are generated. For electrical detection or current generation to occur, the bound excitons must be dissociated into their constituent electrons and holes. Such a process can be induced by the built-in electric field, but the efficiency at the electric fields typically found in organic devices ($F \sim 10^6$ V/cm) is low. The most efficient exciton dissociation in organic materials occurs at a donor-acceptor (D-A) interface. At such an interface, the donor material with a low ionization potential forms a heterojunction with an acceptor material with a high electron affinity. Depending on the alignment of the energy levels of the donor and acceptor materials, the dissociation of the exciton can become energetically favorable at such an interface, leading to a free electron polaron in the acceptor material and a free hole polaron in the donor material.

[023] Organic PV cells have many potential advantages when compared to traditional silicon-based devices. Organic PV cells are light weight, economical in materials use, and can be deposited on low cost substrates, such as flexible plastic foils. However, organic PV devices typically have relatively low quantum yield (the ratio of photons absorbed to carrier pairs generated, or electromagnetic radiation to electricity conversion efficiency), being on the order of 1 % or less. This is, in part,

thought to be due to the second order nature of the intrinsic photoconductive process. That is, carrier generation requires exciton generation, diffusion and ionization or collection. There is an efficiency γ associated with each of these processes. Subscripts may be used as follows: P for power efficiency, EXT for external quantum efficiency, A for photon absorption , ED for diffusion, CC for collection, and INT for internal quantum efficiency. Using this notation:

$$\gamma_P \sim \gamma_{EXT} = \gamma_A * \gamma_{ED} * \gamma_{CC}$$

$$\gamma_{EXT} = \gamma_A * \gamma_{INT}$$

[024] The diffusion length (L_D) of an exciton is typically much less ($L_D \sim 50\Delta$) than the optical absorption length (~500Δ), requiring a trade-off between using a thick, and therefore resistive, cell with multiple or highly folded interfaces, or a thin cell with a low optical absorption efficiency.

[025] The falloff in intensity of an incident flux of electromagnetic radiation through a homogenous absorbing medium is generally given by $I=I_0e^{-\alpha x}$ where I_0 is the intensity at an initial position (X-0), α is the absorption constant and x is the depth from x=0. Thus, the intensity decreases exponentially as the flux progresses through the medium. Accordingly, more light is absorbed with a greater thickness of absorbent media or if the absorption constant can be increased. Generally, the absorption constant for a given photoconductive medium is not adjustable. For certain photoconductive materials, e.g., 3,4,9,10 perylenetetracarboxylic-bis-benzimidazole (PTCBI), or copper phthalocyanine (CuPc), very thick layers are undesirable due to high bulk resistivities.

[026] By suitably re-reflecting or recycling light several times through a given thin film of photoconductive material the optical path through a given photoconductive material can be substantially increased without incurring substantial additional bulk resistance. A solution is needed, which efficiently permits electromagnetic flux to be collected and delivered to the cavity containing the photoconductive material while also confining the delivered flux to the cavity so that it can absorbed.

[027] Less expensive and more efficient devices for photogeneration of power have been sought to make solar power competitive with presently cheaper fossil fuels. Organic photoconductors, such as CuPc and PTCBI, have been sought as materials for organic photovoltaic devices (OPVs) due to potential cost savings. The high bulk resistivities noted above make it desirable to utilize relatively thin films of these materials. However, the use of very thin organic photosensitive layers presents other obstacles to production of an efficient device. As explained above, very thin photosensitive layers absorb a small fraction of incident radiation thus keeping down external quantum efficiency.

[028] Another problem is that very thin films are more subject to defects such as shorts from incursion of the electrode material. U.S. Patent No. 6,333,458, incorporated herein by reference, describes photosensitive heterostructures incorporating one or more exciton blocking layers which address some of the problems with very thin film OPVs. However, other solutions are needed to address the problem of low photoabsorption by very thin films, whether the films are organic or inorganic photoconductors.

[029] The use of optical concentrators, as known as Winston collectors is common in the field of solar energy conversion. Such concentrators have been used primarily in thermal solar collection devices wherein a high thermal gradient is desired. To a lesser extent, they have been used with photovoltaic solar conversion devices. However, it is thought that such applications have been directed to devices wherein photoabsorption was expected to occur upon initial incidence of light upon the active photoconductive medium. If very thin photoconductor layers are used, it is likely that much of the concentrated radiation will not be absorbed. It may be reflected back into the device environment, absorbed by the substrate or merely pass through if the substrate is transparent. Thus, the use of concentrators alone does not address the problem of low photoabsorption by thin photoconductive layers. Optical concentrators for radiation detection have also been used for the detection of Cerenkov or other radiation with photomultiplier ("PM") tubes. PM tubes operate on an entirely different principle, i.e., the photoelectric effect, from solid state detectors such as the OPVs of the present invention. In a PM tube, low photoabsorption in the photoabsorbing medium, i.e., a metallic electrode, is not a concern, but PM tubes require high operating voltages unlike the OPVs disclosed herein.

[030] Light focusing and trapping is an important avenue to increasing the performance of thin film photovoltaic solar cells and photodetectors. However, the mirrors typically used in such schemes utilize metals, such as silver or gold, which can result in significant loss of incident photons due to spectral absorption of the mirror. Thus, it would be advantageous to provide a structure to increase the light-trapping in a

thin film photovoltaic solar cell or photodetector with reduced losses across a large spectral range.

[031] The Inventors have recently demonstrated that growth via molecular beam epitaxy (MBE) of thin, high-efficiency III-V semiconductor solar cells that were "lifted off" from the costly, parent substrate following epitaxial growth. Such a process is significantly different from conventional ELO technologies employed over the last two decades in that "protection layers" were grown surrounding the "sacrificial ELO layer" that is typically etched away to part the active device epitaxy (~2 μm thick) from the parent substrate. This process is described in U.S. Patent Application No. 13/099,850, which is herein incorporated by reference in its entirety. By using a composite protection layer structure both chemical and surface morphological degradation of the parent wafer are eliminated as shown in Figure 1.

[032] Accordingly, the surface of the processed wafer can be made smoother than the starting wafer, and its surface chemistry also remains unchanged, hence removing the need for wafer re-polishing prior to reuse for growth of additional, and also ultimately removable, epitaxial layers. Thus, the parent wafer can be reused indefinitely, as none of the original parent wafer is consumed or altered during the process. Indeed, only the epitaxial active layers that comprise the thin-film, single-crystal, high-efficiency solar cell active region are removed from the entire wafer surface, and subsequently cold-welded (without adhesives that add cost, weight and potential for failure) to a second, thin-film "host" substrate.

[033] Since the substrate is the most costly material used in the process, the multiple-reuse strategy removes the wafer as a material's cost, and transforms its

acquisition into a capital expense, fundamentally changing the cost structure of single crystal III-V-based solar cells. If the very thin, active epitaxial layers of the solar cell are also bonded to a metal or metalized plastic foil without using adhesives, the cost, weight and form factor of the resulting module is also favorably impacted.

[034] In an effort to address at least some of the foregoing described needs, there is disclosed an ultrahigh-efficiency single- and multi-junction thin-film solar cell. The present disclosure is also directed to a substrate-damage-free epitaxial lift-off ("ELO") process that employs adhesive-free, reliable and lightweight cold-weld bonding to a substrate, such as bonding to plastic or metal foils shaped into compound parabolic metal foil concentrators. The Inventors have discovered that combining low-cost solar cell production and ultrahigh-efficiency of solar intensity-concentrated thin-film solar cells on foil substrates shaped into an integrated collector, can result not only in lower cost of the module itself, but also in significant cost reductions in the infrastructure by replacing heavy modules with ultra-lightweight cells on foils (including low-cost integrated concentrators), with power densities exceeding 6 W/gm.

[035] In one embodiment, the present disclosure is directed to a thin-film solar cell comprising a first substrate; a metal contact bonded to said first substrate; an active photovoltaic region bonded to said metal contact; one or more first protection layers; an AlAs layer; one or more second protection layers; and a second substrate, wherein said second substrate.

[036] In another embodiment, the present disclosure is directed to a thin-film solar cell comprising a first substrate; a metal contact bonded to said first substrate; an active photovoltaic region bonded to said metal contact; one or more first protection

layers, wherein at least one of said first protection layers comprise at least one compound chosen from InGaP, GaAs, InGaAs, InP, and InAlP; an AlAs layer; one or more second protection layers, wherein at least one of said second protection layers comprise at least one compound chosen from InGaP, GaAs, InGaAs, InP, and InAlP; and a second substrate, wherein said second substrate comprises at least one compound chosen from GaAs and InP.

[037] In a further embodiment, the present disclosure is directed to a method for performing an epitaxial lift-off process, comprising growing one or more first protection layers on a first substrate; growing an AlAs layer; growing one or more second protection layers; depositing at least one active photovoltaic cell layers on top of the second protection layer; coating the top active photovoltaic cell layer with a metal; coating a second substrate with a metal; pressing together the two metal surfaces to form a cold-weld bond; and removing the AlAs layer with a selective chemical etchant.

[038] In another embodiment, the present disclosure is directed to a method for performing an epitaxial lift-off process, comprising growing one or more first protection layers on a first substrate, wherein at least one of said protection layers comprise a compound chosen from InGaP, GaAs, InGaAs, InP, and InAlP; growing an AlAs layer; growing one or more second protection layers, wherein at least one of said protection layers comprise a compound chosen from InGaP, GaAs, InGaAs, InP, and InAlP; depositing at least one active photovoltaic cell layers on top of the second protection layer; coating the top active photovoltaic cell layer with a metal; coating a second substrate with a metal; pressing together the two metal surfaces to form a cold-weld bond; and removing the AlAs layer with a selective chemical etchant.

[039] Aside from the subject matter discussed above, the present disclosure includes a number of other exemplary features such as those explained hereinafter. It is to be understood that both the foregoing description and the following description are exemplary only.

[040] The accompanying figures are incorporated in, and constitute a part of, this specification.

[041] **Fig. 1.** Is a schematic showing the ELO process according to the present disclosure for InP based solar cells.

[042] **Fig. 2.** Is a photograph of a two inch InP epitaxial layer lifted off and bonded to a Au-coated Kaption sheet. ITO contacts form the Schotty solar cells.

[043] **Fig. 3.** Is an atomic force microscope image of the original epi-ready InP substrate and recovered surfaces after the first and second ELO processes, with and without the use of protection layers.

[044] **Fig. 4.** Is test data and a representative GaAs PV cell layer structure showing cell parameters.

[045] **Fig. 5.** Is test data showing fourth quadrant current voltage and external quantum efficiency (inset) of a 23.9% efficient first-growth cell and a 22.8% efficient cell grown on a reused wafer.

[046] **Fig. 6.** Is a schematic showing the ELO process as applied to an InP material according to the present disclosure.

[047] **Fig. 7.** Is a schematic of a trilayer protection scheme with AlAs layer and AlAs lift-off layer.

[048] **Fig. 8.** Is a schematic of a proposed multi-junction cell structure according to the present disclosure.

[049] **Fig. 9.** Is a schematic of (a) conventional N/P tunnel junctions, and (b) N/ErP/P junction showing the reduced tunneling barriers.

[050] **Fig. 10.** Is a schematic of an integrated reflector with cold-welded bonded ELO multi-junction cell.

[051] One embodiment of the ELO process is shown schematically in Fig. 1. It begins with the epitaxial growth of the chemically distinct, thin "protection layers" consisting of InGaAs and InP, a sacrificial layer of AlAs, a second set of protection layers of InP and InGaAs, and finally the active photovoltaic cell layers. Next, the top epitaxial layer is coated with Au, as is a very thin plastic (e.g. Kapton™, a polyimide film marked by DuPont) host substrate. By pressing the two clean Au surfaces together at only a few kPa pressure, they form an electronically continuous and permanent, adhesive-free cold-weld bond whose properties are indistinguishable from a single, bulk Au film.

[052] Once bonded to the plastic handle, the wafer is ready for ELO. The cold-weld bond is used not only for the ELO process (the epi-layer is attached permanently to the foil substrate prior to the liftoff, peeling away the parent substrate for eventual reuse) but also as the adhesive to the new host substrate on which the solar cells are eventually fabricated.

[053] Replacement of adhesives conventionally used in lift-off by the cold-weld has several benefits: (i) attachment to the foil substrate is simple and is an integral part of the fabrication sequence, (ii) it is lightweight as it completely eliminates an

adhesive layer, (iii) it is thermally and electrical "transparent" since the cold-weld interface is indistinguishable from the bulk of the film, and (iv) it is robust and resistant to failure. A selective chemical etchant, such as HF: H_2O, 1:10, is used to remove the 4 nm to 10 nm-thick AlAs sacrificial ELO layer, parting the entire wafer from the photovoltaic epitaxial layers, leaving the protection layers exposed. The purpose of the protection layer nearest the AlAs ELO layer (InP in this case) is to provide an etch selectivity $>10^8$:1 and is removed from both the substrate and the parted epitaxial layers with a second wet etch ($HCl:H_3PO_4$, 3:1) that stops at the InGaAs protection layer surface. The requirements of the second protection layer are that it can be removed with a wet etchant that stops abruptly at the InP substrate. The InGaAs layer is removed from the wafer using $H_2SO_4:H_2O_2:H_2O$ (1:1:10), followed by $C_6H_8O_7:H_2O_2$ (20:1), both of which have high selectivity to the InP substrate, InP buffer, and epitaxial layers, and assist in the removal of any debris or asperities remaining after the previous etch. Solar cells are fabricated on the epitaxial layers that are attached to the Kapton™ handle by sputtering indium tin oxide (ITO) Schottky contacts. The resulting flexible InP-ITO Schottky solar cells with efficiencies of ~15% under 1 sun AM1.5G illumination are shown in Fig. 2. These bonded epitaxial sheets have been repeatedly cycled to >200 °C without delamination.

[054] Previous to subsequent growth, the substrate is solvent cleaned, an intentional oxide is grown via exposure to UV/Ozone, and then returned to the growth chamber. The process has been employed multiple times with a single substrate to demonstrate degradation-free reuse of InP wafers, and as shown in Fig. 3, the

smoothness of the surface can be improved over that of the commercial epi-ready wafers that are initially used, in principle allowing for indefinite reuse.

[055] The Inventors have recently extended this damage-free regrowth process to GaAs-based single *p-n* junction photovoltaic cells fabricated on a parent wafer, resulting in efficiencies of 23.9%. Fig. 4 is a schematic representation of such a cell. The lift-off process is similar to that used for the InP cells, although the two-protection-layer scheme used for InP is replaced by a three-layer (InGaP/GaAs/InGaP), fully lattice-matched (to the AlAs sacrificial layer) system. This allows for improved etch-selectivity between layers while eliminating debris or surface roughening incurred in the ELO process. The AlAs layer is removed in HF, followed by removal of the InGaP and GaAs protection layers with $HCl:H_3PO_4$ (1:1) and $H_3PO_4:H_2O_2:H_2O$ (3:1:25), respectively.

[056] Following this process, a second cell is grown on the parent wafer, reaching an efficiency of 22.8%. The slight (1%) reduction in power conversion efficiency between the first and second growths is due to the choice of the dry mesa-isolation etch recipe, resulting in a slight reduction in fill factor (see Fig. 4). Furthermore, the anti-reflection coating thickness was not optimal, reducing the external quantum efficiency and short circuit current as shown in Fig. 5. However, even higher efficiencies, for example greater than 25%, are expected when the coating thickness is optimized.

[057] In one embodiment, a protection layer scheme based on the fully lattice-matched InGaP/GaAs/InGaP trilayer can be used. This tri-layer affords etch chemistries with sufficient rate selectivity between layers required to reproducibly remove the

protection layers and to expose a pristine (physically and chemically undamaged) surface. In one embodiment, regrown thin-film cells are bonded via cold-welding to Au-coated plastic (Kapton^{TM}) substrates. It has been shown that a PCE=23.9% for a first growth wafer, and PCE=22.8% for a reused wafer can be achieved, which exceeds the Next Generation Photovoltaics II metric of 20% (see Fig. 5). A depiction of the actual ELO process apparatus and method are shown in Fig. 6.

[058] Following each reuse, both the parent wafer and the lifted off epitaxial layers can be thoroughly studied for damage or subtle degradation. These methods include x-ray photoelectron spectroscopy (XPS) to determine chemical changes to the growth and regrowth surfaces, atomic force microscopy, scanning electron microscopy, and surface profilometry to determine surface morphological changes, cross-sectional transmission electron microscopy to examine defects that are incurred within the bulk of the epitaxy, and compositional depth profiling using secondary ion mass spectroscopy (SIMS).

[059] Completed cells, including anti-reflection coating, can also be electrically tested using standard illumination conditions (1 sun, AM1.5G spectrum). Parameters to be measured include PCE, fill factor (FF), open circuit voltage (Voc), short circuit current (Jsc), series and parallel resistance.

[060] It has been found that extended exposure (>2 days) of Ga-containing compounds (i.e. GaAs, and to a lesser degree InGaP) to HF results in surface contamination that is difficult to remove. This reaction, however, is absent for InP surfaces exposed to HF for over 7 days. In one embodiment a thin layer of strained InP

placed immediately below the AlAs sacrificial layer will improve the fidelity of the surface, as shown in Fig. 7.

[061] The thickness of the InP is limited to prevent strain relaxation, which can degrade the subsequently grown PV layer quality. The critical thickness of InP on GaAs is between 5 and 6 monolayers, corresponding to ~1.7 nm. In this case the protection layer scheme would comprise InGaP/GaAs/InP or InGaP/GaAs/InGaP/InP, where the additional InGaP layer in the latter structure provides improved protection above the GaAs.

[062] In another embodiment, the etch selectivity and preservation of the as-purchased wafer quality is carried out by using additional materials combinations, for example by replacing the InGaP layer adjacent to the InAlP. An InAlP/InGaP/GaAs/InAlP structure may be advantageous since InAlP can be etched with $HCl:H_2O$ (1:5), which stops abruptly at GaAs (>400:1 etch ratio), whereas $HCl:H_3PO_4$(1:1) used to etch InGaP slowly attacks the GaAs which results in roughening. By placing the InAlP adjacent to the AlAs layer, the InAlP is attacked by the HF and reduces the buildup of arsenic oxide which can slow the liftoff process. Also, InGaP may be used as an etch stop for the GaAs etch ($H_3PO_4:H_2O_2:H_2O$, 3:1:25) to ensure that the lower InAlP layer is only removed in the final etch step.

[063] Additional cost reduction may be possible by bonding to metal-foil substrates such as Au-coated Cu foils, use of less expensive metals for cold-welding (e.g. Ag instead of Au), reduced consumption of HF, reduced protection layer thicknesses, and accelerating the lift-off process. The extended exposure to HF used to dissolve the AlAs sacrificial layer limits the choice of metal host substrates that can be

employed. In one embodiment, Cu foils, which can be used for cold-welding, are used to increase resistance upon exposure to HF, as their use may be simpler than coating the foil with a noble metal such as Au. An additional benefit to using Cu foil is its high thermal conductivity (~4W $cm^{-1}{}^{\circ}C^{-1}$) that can be exploited to extract heat from the concentrated cells.

[064] There is also disclosed very high-efficiency multi-junction (GaAs/InGaP) solar cells following the two cell example structure shown in Fig. 8.

[065] The design is inverted relative to a conventional multi-junction cell growth sequence to accommodate the "upside down" bonding geometry used in the adhesive-free cold-weld process; the structure includes a 25% GaAs cell architecture. In this case, the GaAs cell thickness is reduced to 2 μm (50% of the conventional substrate-based cell) since the reflective, full-coverage ohmic contact allows for two passes of the incident light through the device active region. The primary focus will be on optimizing the tandem PV structure for maximum efficiency, including InGaP cell design (layer thickness, window layer, layer composition, etc.), improving the wide-gap tunnel junctions (TJ) between elements in the stack, and perfecting the multiple lift-off process over large areas for this multi-junction cell.

[066] Solar cells will be grown with *n*-type material *on top of* *p*-type layers, whereas the tunnel junctions must be grown with the opposite polarity. The cells may employ carbon-doping in all or several of the *p*-type layers, since carbon does not readily migrate to the growth surface as does the conventional *p*-dopant, Be. As the tandem cells are generally limited by the current in the GaAs cell, the InGaP cell

thickness needs to be adjusted to current-match the InGaP and GaAs cells; the thickness of the InGaP layer is expected to range from 0.55 to 0.80 μm.

[067] Efficient tunnel junctions (TJ) are essential for high performance tandem cells. They need to be nearly loss-less in both voltage and absorption. It is advantageous to use an InGaP TJ in MJ cells to avoid GaAs TJ absorption that may be as high as 3%. A conventional TJ is an abrupt *P+/N+* junction where the electron can tunnel directly from the conduction band on the *n*-type side to the valence band on the *p*-type side (Fig.9(a)). Little work has been performed on MBE grown wide gap TJs, although doping levels that are sufficiently high to transport currents generated at 1 sun illumination have been reported using MBE.

[068] One embodiment is directed to InGaP tunnel junctions that have a voltage drop of several tens of mV at 1 sun. Research suggests that Be and Si are suitable dopants (attaining densities of $3.7x10^{19}$ and $1.8x10^{19}$ cm^{-3}, respectively). However, if a reduced tunneling resistance is required, the use of engineered defects at the *P+/N+* interface, can be done, such as by adding ErAs to a GaAs tunnel junction. In this case, ErP or LuP may be used as shown in Fig. 9b. The ErP or LuP form epitaxial islands on the semiconductor surface that are ~ 4 monolayers thick, are metallic, and split the tunneling process into two steps with significantly higher tunneling probabilities. By employing ErP in the TJ, several orders of magnitude increase in the tunneling current may result, and lead to voltage drops in the sub-mV range for the currents anticipated in the fabricated PV cells.

[069] As in the case of the single junction cells, the multi-junction cell can be microscopically and chemically examined after each iteration of the growth-ELO-reuse

cycle. Completed cells, including anti-reflection coating, can be electrically tested using standard illumination conditions (AM1.5G spectrum), but over a range of intensities up to 10 suns. Parameters to be measured include PCE, fill factor, open circuit voltage, short circuit current, series and parallel resistance, as in the case of the single junction cells.

[070] Thin-film multi-junction cells bonded onto reflective and flexible substrates provide a unique opportunity to integrate the solar collector with the thin-film cell without introducing significant additional costs. Fig. 10 shows that a strip consisting of the ELO multi-junction cell is bonded to the center of a larger, flexible, reflective film. The film is then molded (by placement in a thermally conductive or actively cooled preform) into the shape of a compound parabolic collector (e.g. a CPC, or Winston collector). This geometry concentrates parallel solar rays onto the cell strip at its focus, as well as collects diffuse light within the acceptance cone.

[071] The small levels of concentration (4-10X) generally used in the cylindrical Winston-type collectors allow the concentrators to be highly efficient, and to direct a significant amount to diffuse light into the cell. The efficiency of collection is given by $CEff=T_{CPC}\gamma$, where T_{CPC} is the effective transmittance of the CPC, including losses of multiple bounces that are ~2% for common reflector materials. The correction for diffuse light is $\gamma=1-(1-1/C)Gdiff/Gdir$, where C is the intended concentration, and Gdiff/Gdir is the fraction of diffuse to total incident light. Typically, Gdiff/Gdir~0.11 for a low-cloudiness day. Then for C=4, $\gamma=90\%$ at AM1.5G, which is comparable to the power available at AM1.5D.

[072] For a 4X CPC, and assuming a solar cell strip width of 1 cm, the aperture is then 4 cm wide x 10 cm deep, providing a practical form factor compatible with panels used in single family dwellings. At higher concentrations, the size of the concentrator increases considerably. For example, a 10X concentration used with the same 1 cm wide cell strip requires an aperture of 10cm with a depth of ~ 55cm. This can be reduced to ~40cm with negligible effect on concentration efficiency. [25] The amount of reflective material needed is 4-5 times larger for 4X concentration, and 8-11 times for 10X concentration.

[073] Additional benefits to the small concentrations used include the allowed use of single-axis tracking (daily or seasonally, depending on orientation of the collector), and simplified passive cooling than are needed for higher concentrations. Indeed, the very thin substrates used greatly simplify heat transfer: calculations indicate that at 10X concentration and a 25mm thick Kapton™ substrate placed against a passively cooled Cu heat sink results in a temperature rise of only 5-20°C, obviating the need for more aggressive cooling methods.

[074] Note that the ELO cell technology can also be applied to systems with large concentration factors; however, here the present disclosure focused only on smaller concentrations that lead to simple and economical designs that are applicable to residential systems. The cost reductions in this integrated solar collector + ELO multi-junction concentrator cell assembly is expected to radically reduce the cost of concentrated systems, as well as their footprint (owing to the high PCE).

[075] Unless otherwise indicated, all numbers expressing quantities of ingredients, reaction conditions, and so forth used in the specification and claims are to

be understood as being modified in all instances by the term “about.” Accordingly, unless indicated to the contrary, the numerical parameters set forth in the following specification and attached claims are approximations that may vary depending upon the desired properties sought to be obtained by the present invention.

[076] Other embodiments of the invention will be apparent to those skilled in the art from consideration of the specification and practice of the invention disclosed herein. It is intended that the specification and examples be considered as exemplary only, with the true scope of the invention being indicated by the following claims.

What Is Claimed Is:

1. A thin-film solar cell comprising:

a first substrate;

a metal contact bonded to said first substrate;

an active photovoltaic region bonded to said metal contact;

one or more first protection layers, wherein at least one of said first protection layers comprise at least one compound chosen from InGaP, GaAs, InGaAs, InP, and InAlP;

an AlAs layer;

one or more second protection layers, wherein at least one of said second protection layers comprise at least one compound chosen from InGaP, GaAs, InGaAs, InP, and InAlP;

and a second substrate, wherein said second substrate comprises at least one compound chosen from GaAs and InP.

2. The thin-film solar cell according to claim 1, wherein said thin-film solar cell comprises two first and/or second protection layers.

3. The thin-film solar cell according to claim 1, wherein said thin-film solar cell comprises three first and/or second protection layers.

4. The thin-film solar cell according to claim 1, wherein said first substrate comprises a plastic or a metal foil.

5. The thin-film solar cell according to claim 4, wherein said first substrate comprises a polyimide film.

6. The thin-film solar cell according to claim 1, wherein said metal contact comprises at least one metal chosen from Au, Ag, and Cu.

7. The thin-film solar cell according to claim 6, wherein said metal contact comprises Au.

8. The thin-film solar cell according to claim 6, wherein said metal contact comprises Cu.

9. The thin-film solar cell according to claim 1, wherein said thin-film solar cell is integrated into a solar collector, wherein said solar collector is molded into a shape chosen from a compound parabolic collector or a Winston collector.

10. A method for performing an epitaxial lift-off process, comprising:

growing one or more first protection layers on a first substrate, wherein at least one of said protection layers comprise a compound chosen from InGaP, GaAs, InGaAs, InP, and InAlP;

growing an AlAs layer;

growing one or more second protection layers, wherein at least one of said protection layers comprise a compound chosen from InGaP, GaAs, InGaAs, InP, and InAlP;

depositing at least one active photovoltaic cell layers on top of the second protection layer;

coating the top active photovoltaic cell layer with a metal;

coating a second substrate with a metal;

pressing together the two metal surfaces to form a cold-weld bond;

and removing the AlAs layer with a selective chemical etchant.

11. The method of claim 10, wherein each additional protection layer is removed with a selective chemical etchant.

12. The method of claim 11, wherein the first substrate is solvent cleaned and treated to form an oxide layer.

13. The method of claim 10, wherein the second substrate is chosen from a plastic or a metal foil.

14. The method of claim 13, wherein the second substrate is chosen from a polyimide film.

15. The method of claim 10, wherein said metal contact comprises at least one metal chosen from Au, Ag, and Cu.

16. The method of claim 15, wherein said metal contact comprises Au.

17. The method of claim 15, wherein said metal contact comprises Cu.

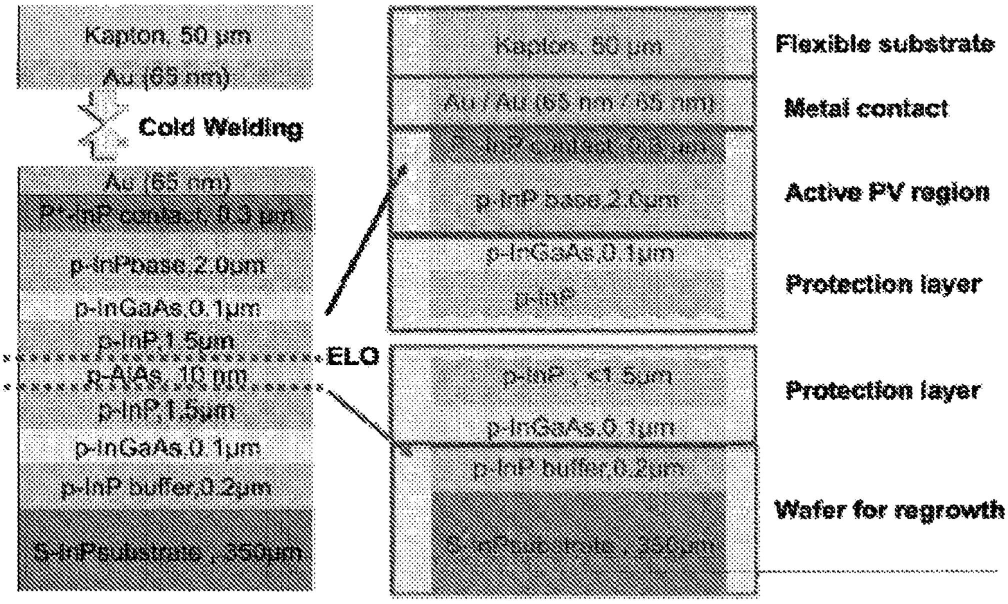
Kapton, 50 µm
Au (65 nm)
Cold Welding
Au (65 nm)
P+-InP contact, 0.3 µm
p-InPbase,2.0µm
p-InGaAs,0.1µm
p-InP,1.5µm
p-AlAs, 10 nm
p-InP,1.5µm
p-InGaAs,0.1µm
p-InP buffer,0.2µm
S-InPsubstrate, 350µm
ELO
Kapton, 50 µm
Au / Au (65 nm / 65 nm)
P+-InP contact, 0.3 µm
p-InP base,2.0µm
p-InGaAs,0.1µm
p-InP
p-InP, <1.5µm
p-InGaAs,0.1µm
p-InP buffer,0.2µm
S-InPsubstrate, 350µm
Flexible substrate
Metal contact
Active PV region
Protection layer
Protection layer
Wafer for regrowth

Fig. 1

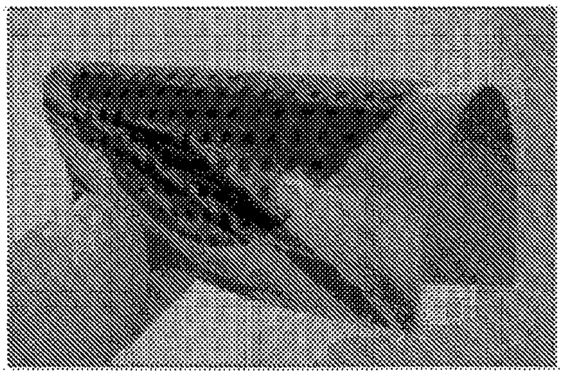

Fig. 2

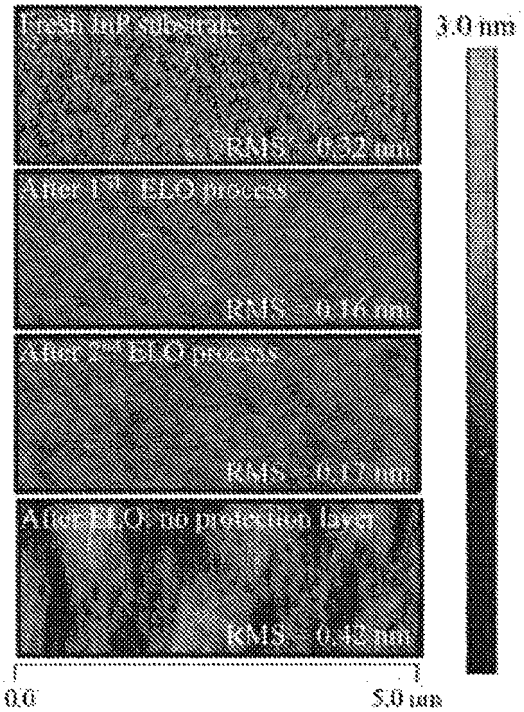

Fig. 3

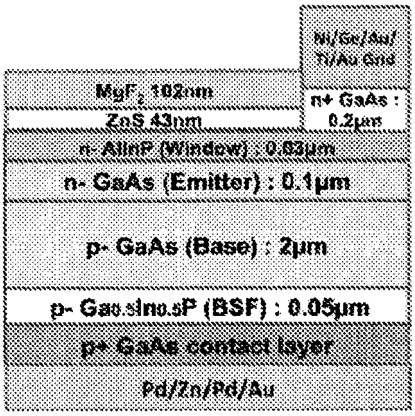

	Jsc[mA-cm^2]	Voc [V]	FF	η_P
Fresh	28.2	1.01	84.4%	23.9%
Reused	27.7	1.01	81.6%	22.8%

Fig. 4

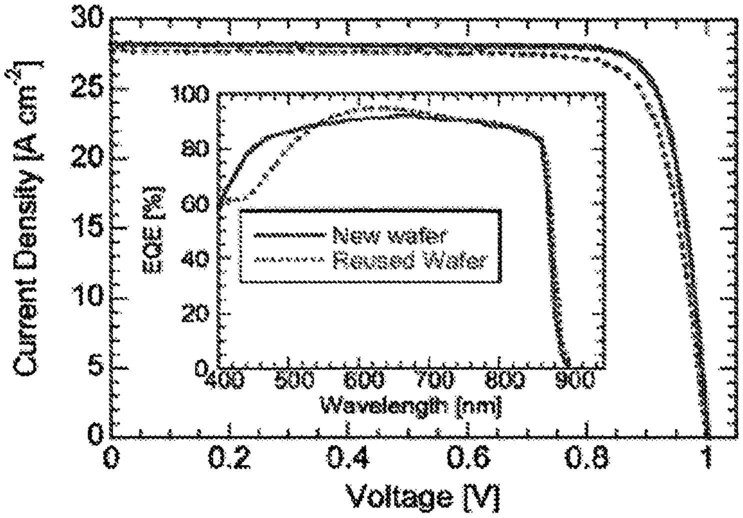
Current Density [A cm^{-2}]
30
25
20
15
10
5
0
0
0.2
0.4
0.6
0.8
1
Voltage [V]
EQE [%]
100
80
60
40
20
0
400
500
600
700
800
900
Wavelength [nm]
New wafer
Reused Wafer

Fig. 5

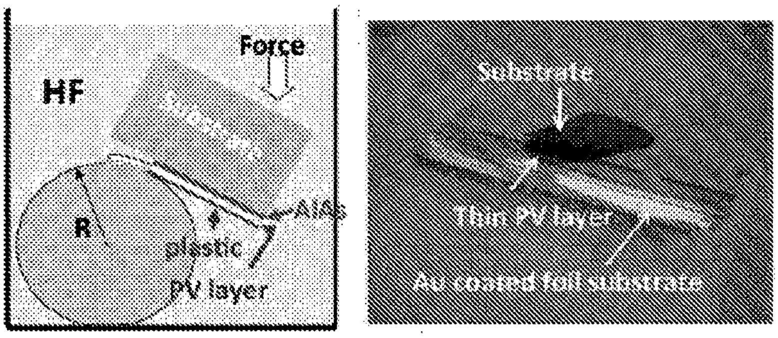
HF
Force
Substrate
AlAs
R
plastic
PV layer
Substrate
Thin PV layer
Au coated foil substrate

Fig. 6

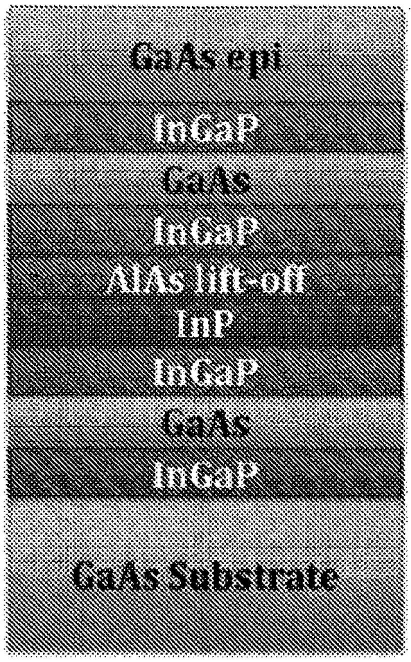
GaAs epi
InGaP
GaAs
InGaP
AlAs lift-off
InP
InGaP
GaAs
InGaP
GaAs Substrate

Fig. 7

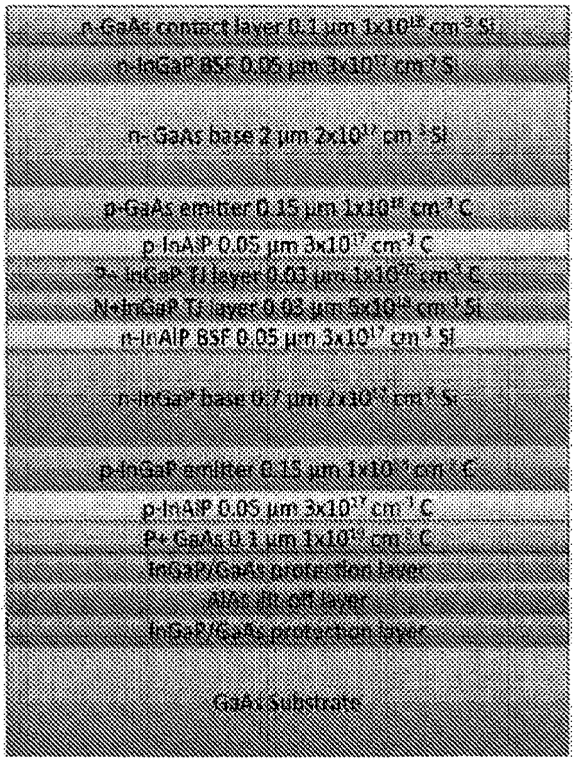
n-GaAs contact layer 0.1 µm 1x10^{18} cm^{-3} Si
n-InGaP BSF 0.05 µm 3x10^{17} cm^{-3} Si
n- GaAs base 2 µm 2x10^{17} cm^{-3} Si
p-GaAs emitter 0.15 µm 1x10^{18} cm^{-3} C
p-InAlP 0.05 µm 3x10^{17} cm^{-3} C
P+ InGaP TJ layer 0.03 µm 1x10^{20} cm^{-3} C
N+InGaP TJ layer 0.03 µm 5x10^{19} cm^{-3} Si
n-InAlP BSF 0.05 µm 3x10^{17} cm^{-3} Si
n-InGaP base 0.7 µm 2x10^{17} cm^{-3} Si
p-InGaP emitter 0.15 µm 1x10^{18} cm^{-3} C
p-InAlP 0.05 µm 3x10^{17} cm^{-3} C
P+ GaAs 0.1 µm 1x10^{19} cm^{-3} C
InGaP/GaAs protection layer
AlAs lift-off layer
InGaP/GaAs protection layer
GaAs Substrate

Fig. 8

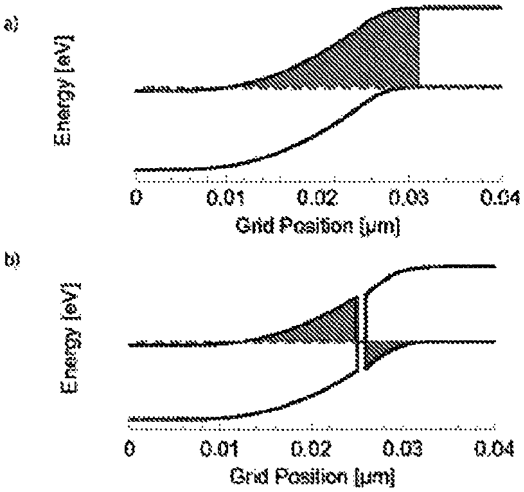
a)
Energy [eV]
0
0.01
0.02
0.03
0.04
Grid Position [μm]
b)
Energy [eV]
0
0.01
0.02
0.03
0.04
Grid Position [μm]

Fig. 9

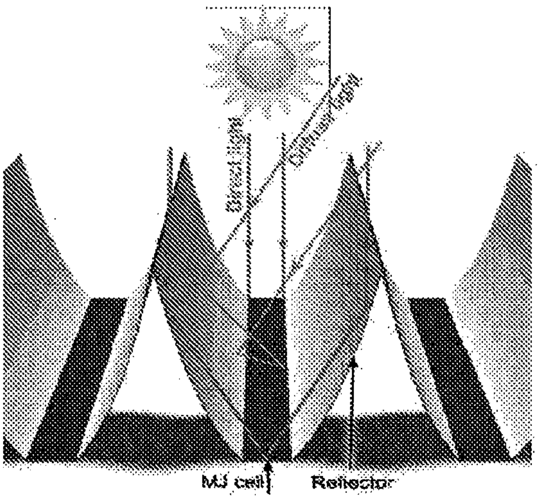
Direct light
Diffuse light
MJ cell
Reflector

Fig. 10

(19) 中华人民共和国国家知识产权局

(12) 发明专利申请

(10) 申请公布号 CN 103890974 A
(43) 申请公布日 2014.06.25

(21) 申请号 201280042064.7

(22) 申请日 2012.07.06

(30) 优先权数据
61/505,014 2011.07.06 US

(85) PCT国际申请进入国家阶段日
2014.02.27

(86) PCT国际申请的申请数据
PCT/US2012/045778 2012.07.06

(87) PCT国际申请的公布数据
WO2013/006803 EN 2013.01.10

(71) 申请人 密歇根大学董事会
地址 美国密歇根州

(72) 发明人 史蒂芬·R·福里斯特
克里斯多佛·凯尔·伦肖
迈克尔·斯洛特斯基

(74) 专利代理机构 中原信达知识产权代理有限责任公司 11219
代理人 韩峰　孙志湧

(51) Int. Cl.
H01L 31/18 (2006.01)
H01L 31/0687 (2006.01)
H01L 31/0693 (2006.01)
H01L 31/0304 (2006.01)
H01L 21/78 (2006.01)

权利要求书2页　说明书10页　附图4页

(54) 发明名称

使用外延剥离和冷焊结合的半导体太阳能电池的集成太阳能收集器

(57) 摘要

公开了一种超高效的单结和多结薄膜太阳能电池。本公开还涉及基板无损伤外延剥离(ELO)工艺，其对于基板采用无粘合剂、可靠且轻质的冷焊结合，诸如对于成形为复合抛物线金属箔聚能器的塑料或金属箔的结合。通过如本文所述地将低成本天阳能电池生产和在箔基板上被成形为集成收集器的会聚太阳能强度的薄膜太阳能电池的超高效率相结合，实现了更低成本的模块以及基础结构的显著成本降低。

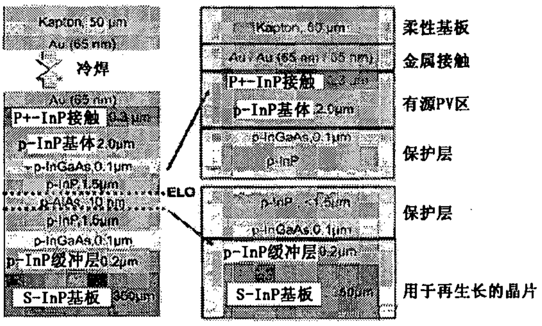

1. 一种薄膜太阳能电池，包括：

第一基板；

金属接触，所述金属接触被结合到所述第一基板；

有源光伏区，所述有源光伏区被结合到所述金属接触；

一个或多个第一保护层，其中，所述第一保护层中的至少一个第一保护层包括从InGaP、GaAs、InGaAs、InP和InAlP中选择的至少一种化合物；

AlAs层；

一个或多个第二保护层，其中，所述第二保护层中的至少一个第二保护层包括从InGaP、GaAs、InGaAs、InP和InAlP中选择的至少一种化合物；以及

第二基板，其中，所述第二基板包括从GaAs和InP中选择的至少一种化合物。

2. 根据权利要求1所述的薄膜太阳能电池，其中，所述薄膜太阳能电池包括两个第一和/或第二保护层。

3. 根据权利要求1所述的薄膜太阳能电池，其中，所述薄膜太阳能电池包括三个第一和/或第二保护层。

4. 根据权利要求1所述的薄膜太阳能电池，其中，所述第一基板包括塑料或金属箔。

5. 根据权利要求4所述的薄膜太阳能电池，其中，所述第一基板包括聚酰亚胺膜。

6. 根据权利要求1所述的薄膜太阳能电池，其中，所述金属接触包括从Au、Ag和Cu中选择的至少一种金属。

7. 根据权利要求6所述的薄膜太阳能电池，其中，所述金属接触包括Au。

8. 根据权利要求6所述的薄膜太阳能电池，其中，所述金属接触包括Cu。

9. 根据权利要求1所述的薄膜太阳能电池，其中，所述薄膜太阳能电池被集成到太阳能收集器中，其中，所述太阳能收集器被模制成从复合抛物线收集器或温斯顿收集器中选择的形状。

10. 一种执行外延剥离工艺的方法，包括：

在第一基板上生长一个或多个第一保护层，其中，该保护层中的至少一个保护层包括从InGaP、GaAs、InGaAs、InP和InAlP中选择的化合物；

生长AlAs层；

生长一个或多个第二保护层，其中，该保护层中的至少一个保护层包括从InGaP、GaAs、InGaAs、InP和InAlP中选择的化合物；

在所述第二保护层的顶部上沉积至少一个有源光伏电池层；

利用金属涂敷顶部的有源光伏电池层；

利用金属涂敷第二基板；

将两个金属表面压到一起，以形成冷焊结合；以及，

利用选择性化学蚀刻剂去除所述AlAs层。

11. 根据权利要求10所述的方法，其中，利用选择性化学蚀刻剂去除每个附加的保护层。

12. 根据权利要求11所述的方法，其中，所述第一基板被用溶剂清洁和处理以形成氧化物层。

13. 根据权利要求10所述的方法，其中，所述第二基板选自塑料或金属箔。

14. 根据权利要求13所述的方法，其中，所述第二基板选自聚酰亚胺膜。

15. 根据权利要求10所述的方法，其中，所述金属接触包括从Au、Ag和Cu中选择的至少一种金属。

16. 根据权利要求15所述的方法，其中，所述金属接触包括Au。

17. 根据权利要求15所述的方法，其中，所述金属接触包括Cu。

使用外延剥离和冷焊结合的半导体太阳能电池的集成太阳能收集器

[0001] 相关申请的交叉应用

[0002] 本申请要求2011年7月6日提交的美国临时申请No.61/505,014的权益，该临时申请的全文以引用方式并入本文。

[0003] 联合研究协议

[0004] 要求保护的发明是根据大学-公司联合研究协议由下列团体中一个或多个做出，并代表其名义和/或与其相关：密歇根大学和环球光子能量公司(Global Photonic Energy Corporation)。该协议在发明做出之时和之前有效，并且在该协议范围内进行的研究获得要求保护的发明。

技术领域

[0005] 本公开涉及超高效率的单结和多结薄膜太阳能电池。本发明还涉及基板无损伤外延剥离(ELO)工艺，其对于基板采用无粘合剂、可靠和质轻的冷焊结合，诸如对于成形为复合抛物线金属箔聚能器的塑料或金属箔的结合。

背景技术

[0006] 光电子器件依赖于材料的光学性质和电子性质，以用电子学方法来产生或检测电磁辐射或者由环境电磁辐射产生电力。

[0007] 光敏光电子器件将电磁辐射转换成电力。太阳能电池、也称为光伏(PV)器件，是一类专门用于产生电能的光敏光电子器件。可以用太阳光之外的光源产生电能的PV器件可以用于驱动耗电负载以提供例如照明、加热，或为诸如计算器、无线电、计算机或远程监测或通信设备的电子电路或装置供电。这些发电应用通常还涉及电池或其他能量存储装置的充电，使得当来自太阳或其他光源的直接照射不可用时能够继续运行，或根据特定应用的要求平衡PV器件的电力输出。当在本文中使用时，术语“电阻性负载”是指任何耗电或储电电路、装置、设备或系统。

[0008] 另一种类型的光敏光电子器件是光电导体电池。在这种功能中，信号检测电路监测器件的电阻以检测由光的吸收所引起的变化。

[0009] 另一种类型的光敏光电子器件是光电检测器。在操作中，光电检测器与电流检测电路结合使用，该电流检测电路测量当光电检测器暴露于电磁辐射并可以具有施加的偏置电压时所产生的电流。本文描述的检测电路能够向光电检测器提供偏置电压并且测量光电检测器对电磁辐射的电子响应。

[0010] 这三种类别的光敏光电子器件可以根据是否存在下文定义的整流结并且还根据器件是否使用也称为偏压或偏置电压的外加电压进行操作来表征。光电导体电池没有整流结并且通常使用偏压进行操作。PV器件具有至少一个整流结并且不使用偏压进行操作。光电检测器具有至少一个整流结但通常不总是使用偏压进行操作。按惯例，光伏电池向电路、装置或设备供电，但是不提供信号或电流来控制检测电路或从检测电路输出信息。相比之

下，光电检测器或光电导体提供信号或电流以控制检测电路或从检测电路输出信息，但是不向电路、装置或设备供电。

[0011] 传统上，光敏光电子器件由多种无机半导体构成，例如晶体、多晶和非晶硅、砷化镓、碲化镉等。在本文中，术语“半导体”是指当受到热或电磁激发感生电荷载流子时能够传导电力的材料。术语“光电导”一般是指电磁辐射能量被吸收并且从而转换成电荷载流子的激发能以便载流子能够传导，即传输材料中的电荷的过程。术语“光电导体”和“光电导材料”在本文中用于指由于其为了吸收电磁辐射来产生电荷载流子的性质而被选择的半导体材料。

[0012] PV 器件可以由它们能够将入射太阳能转换成可用电能的效率来表征。利用晶体或非晶硅的器件在商业应用中占主导地位，并且某些已经达到 23% 或更大的效率。然而，有效的基于晶体的器件，特别是大表面积器件，由于在没有明显降低效率的缺陷地生产大晶体中固有的问题，生产起来困难且昂贵。另一方面，高效非晶硅器件仍然受到稳定性问题的困扰。目前可商购的非晶硅电池的稳定转换效率在 4 到 8% 之间。更近的尝试已经聚焦于使用有机光伏电池以经济的生产成本获得可接受的光伏转换效率。

[0013] 可以对 PV 器件进行优化，以在标准照射条件（即，标准测试条件，其为 1000W/m2、AMI.5 光谱照射）下最大化电能产生，用于最大化光电流乘以光电压的乘积。这种电池在标准照射条件下的电能转换效率取决于以下三个参数 :(1) 零偏压下的电流，即短路电流 Isc,，单位为安培 ;(2) 开路条件下的光电压，即开路电压 V_{OC}，单位为伏特 ;以及 (3) 填充因子 ff。

[0014] PV 器件在跨负载连接并用光照射时，产生光生电流。当在无限负载下照射时，PV 器件产生其最大可能电压，$V_{\text{开路电压}}$或 V_{OC}。当在其电接触短路的情况下照射时，PV 器件产生其最大可能电流，$I_{\text{短路电流}}$或 I_{SC}。当实际用于产生电力时，PV 器件连接到有限电阻性负载并且电力输出由电流和电压的乘积 I×V 给出。由 PV 器件产生的最大总电力必然不能超过乘积 $I_{SC}\times V_{OC}$。当对负载值进行优化以获得最大功率提取时，电流和电压分别具有值 I_{max} 和 V_{max}。

[0015] PV 器件的品质因数是填充因子 ff，其定义为 :

[0016] $ff=\{I_{max}\ V_{max}\}/\{I_{SC}\ V_{OC}\}$ (1)

[0017] 其中，ff 总是小于 1，因为在实际使用中永远不能同时获得 I_{SC} 和 V_{OC}。但是，在最佳条件下，当 ff 接近 1 时，器件具有较低的串联或内部电阻，因此向负载提供 I_{SC} 与 V_{OC} 的乘积的更大百分率。当 P_{inc} 是在器件上入射的功率时，器件的功率效率 γ_P 可以由下式计算 :

[0018] $\gamma_P=ff*(I_{SC}*V_{OC})/P_{inc}$

[0019] 当适合能量的电磁辐射入射在例如有机分子晶体（OMC）材料或聚合物的半导体有机材料上时，光子可以被吸收以产生被激发的分子状态。这用符号表示为 $S_0+hv\Psi S_0^*$。这里，S_0 和 S_0^* 分别表示分子的基态和激发态。这种能量吸收伴有电子从可以是 B- 键的 HOMO 能级中的束缚态跃迁到可以是 B^*- 键的 LUMO 能级，或等价地，空穴从 LUMO 能级跃迁到 HOMO 能级。在有机薄膜光电导体中，一般相信产生的分子状态是激子，即作为准粒子传输的处于束缚态的电子 - 空穴对。激子在成对复合之前可以具有可观的寿命，该成对复合是指原始的电子和空穴彼此复合的过程，这与同来自其他对的空穴或电子的复合相反。为了产生光电流，将电子 - 空穴对分离，通常是在两个不同的相接触的有机薄膜之间的施主 - 受主界面

处分离。如果电荷没有分离，则它们可以在也称为淬灭过程的成对复合过程中，辐射地通过发射比入射光的能量更低的光，或非辐射地通过产生热而复合。在光敏光电子器件中，这些结果中的任一种都不是想要的。

[0020] 在接触处的电场或不均匀性会造成激子淬灭而不是在施主-受主界面处游离，导致对电流没有净贡献。因此，期望使光生激子保持远离接触。这具有限制激子向结附近的区域扩散，以便关联电场有更多的机会分离由结附近的激子游离所释放的电荷载流子的作用。

[0021] 为了产生占据显著体积的内生电场，常用的方法是将具有特别是在其分子量子能态分布方面具有适当选择的导电性质的两层材料并置。这两种材料的界面被称为光伏异质结。在传统半导体理论中，用于形成 PV 异质结的材料一般被称为 n 或 p 型。这里 n 型是指多数载流子类型是电子。这可以被视为具有许多处于相对自由能态中的电子的材料。p 型是指多数载流子类型是空穴。这样的材料具有许多处于相对自由能态的空穴。本底的类型，即非光生的多数载流子浓度，主要取决于由缺陷或杂质引起的无意掺杂。杂质的类型和浓度决定了最高占据分子轨道（HOMO）能级与最低未占分子轨道（LUMO）能级之间的能隙（被称为 HOMO-LUMO 能隙）中的费米能量或能级的值。费米能量的特征在于分子量子能态的统计学占据，其用占据概率等于 1/2 时的能量值表示。费米能量接近 LUMO 能级指示电子是优势载流子。费米能量接近 HOMO 能级指示空穴是优势载流子。因此，费米能量是传统半导体的主要定性性质并且原型 PV 异质结传统上是 p-n 界面。

[0022] 术语“整流”尤其是指具有不对称导电特性的界面，即，界面支持优选一个方向上的电子电荷传输。整流一般与适当选择的材料之间的异质结处产生的内建电场相关。

[0023] 当在本文中使用时，并且正如本技术领域的专业人员将通常理解的，如果第一个“最高占据分子轨道”（HOMO）或“最低未占分子轨道”（LUMO）能级更接近真空能级，则第一个能级“大于”或“高于”第二个 HOMO 或 LUMO 能级。由于电离电势（IP）被测量为相对于真空能级的负能量，因此更高的 HOMO 能级对应于具有较小绝对值的 IP（负得较少的 IP）。同样，更高的 LUMO 能级对应于具有更小绝对值的电子亲和势（EA）（负得较少的 EA）。在常规能级图上，真空能级位于顶部，材料的 LUMO 能级高于同一材料的 HOMO 能级。“更高的”HOMO 或 LUMO 能级与“更低的”HOMO 或 LUMO 能级相比，显得更接近于此能级图的顶部。

[0024] 在有机材料的情形下，术语“施主”和“受主”是指两种相接触但是不同的有机材料的 HOMO 能级和 LUMO 能级的相对位置。这与这些术语在无机材料情形中的使用相反，在无机材料情形中，“施主”和“受主”可以是指分别可用于产生无机 n 型层和 ρ 型层的掺杂物的类型。在有机材料情形中，如果与一种材料接触的另一种材料的 LUMO 能级较低，则该材料是受主。否则，它是施主。在不存在外部偏压的情况下，施主-受主结处的电子移动到受主材料中并且空穴移动到施主材料中，在能量上是有利的。

[0025] 有机半导体的显著性质是载流子迁移率。迁移率度量了电荷载流子能够响应于电场通过导电材料移动的容易度。在有机光敏器件的情形中，包括有由于高电子迁移率而倾向于通过电子进行传导的材料的层可以被称为电子传输层或 ETL。包括有由于高空穴迁移率而倾向于通过空穴进行传导的材料的层可以被称为空穴传输层或 HTL。优选地，但不是必须的，受主材料是 ETL 并且施主材料是 HTL。

[0026]　常规的无机半导体 PV 电池采用 p-n 结建立内部电场。早期的有机薄膜电池，诸如 Tang 的 Appl. Phys Lett. 48,183（1986）所报道的，包含与在常规无机 PV 电池中使用的类似的异质结。然而，现在认识到，除了 p-n 型结的建立之外，异质结的能级失谐也发挥重要作用。

[0027]　由于有机材料中光生过程的基本性质，据信，有机 D-A 异质结处的能级失谐对于有机 PV 器件的操作来说是重要的。在有机材料的光学激发后，产生了局部化的弗伦克尔（Frenkel）或电荷转移激子。为了进行电检测或产生电流，必须使束缚的激子游离成它们的组分电子和空穴。这样的过程可以由内建电场感生，但是在有机器件中通常得到的电场（$F \sim 10^6 V/cm$）下的效率低。有机材料中最有效的激子游离发生在施主 - 受主（D-A）界面处。在这种界面处，具有低电离电势的施主材料与具有高电子亲和势的受主材料形成异质结。取决于施主和受主材料的能级排列，激子在这种界面处的游离可能变得能量上有利，从而造成在受主材料中的自由电子极化子以及在施主材料中的自由空穴极化子。

[0028]　有机 PV 电池在与传统的基于硅的器件相比时具有许多潜在优点。有机 PV 电池重量轻，材料的使用经济，并且可以沉积在诸如柔性塑料箔的低成本基板上。然而，有机 PV 器件通常具有相对低的量子产率（所吸收的光子与所产生的载流子的比率、或电磁辐射到电力的转换效率），其在 1% 或更低的量级上。据认为，这部分是由于固有的光电导过程的次级性质导致的。也就是说，载流子产生需要激子的产生、扩散和电离或收集。这些过程中的每一个都伴有效率 γ。下标可以如下使用：P 表示功率效率，EXT 表示外量子效率，A 表示光子吸收，ED 表示扩散，CC 表示收集，并且 INT 表示内量子效率。使用该表示法：

[0029]　$\gamma_P \sim \gamma_{EXT} = \gamma_A * \gamma_{ED} * \gamma_{CC}$

[0030]　$\gamma_{EXT} = \gamma_A * \gamma_{INT}$

[0031]　激子的扩散长度（Ld）（$L_D \sim 50\Delta$）典型情况下远小于光学吸收长度（$\sim 500\Delta$），从而在使用具有多个或高度折叠界面的厚的并因此高电阻的电池或具有低光学吸收效率的薄电池之间，需要折衷。

[0032]　通常用 $I=I_0e^{-\alpha x}$ 给出通过同质吸收介质的电磁辐射的入射通量的强度衰减，其中，I_0 是初始位置（X-0）处的强度，a 是吸收常数并且 x 是距离 x=0 的深度。因此，随着通量穿过介质前进，强度指数地减小。因此，吸收介质的厚度越大或者如果吸收常数可以增大，吸收的光越多。通常，给定光导电介质的吸收常数是不可调的。对于某些光导电材料，例如，3,4,9,10- 二萘嵌苯四羧联二苯并咪唑（PTCBI）或铜酞菁（CuPc），由于高体电阻率，导致非常厚的层是不期望的。

[0033]　通过穿过光导电材料的给定薄膜适当地多次再反射或再循环光，穿过给定光导电材料的光路可以显著增加，而不引起显著的附加体电阻。需要一种解决方案，其有效地允许电磁通量被收集并且传递到包含光导电材料的腔体，同时还将所传递的通量限于腔体，使得其可以被吸收。

[0034]　已经寻求了用于光生功率的更便宜和更有效的器件来使太阳能与目前较便宜的矿物燃料相媲美。由于有可能节省成本，已经寻求到诸如 CuPc 或 PTCBI 的有机光导体作为用于有机光伏器件（OPV）的材料。上述的高体电阻率使得期望的是利用这些材料的相对薄的膜。然而，使用非常薄的有机光敏层对于生成有效装置存在其它阻碍。如以上说明的，非常薄的光敏层吸收一小部分入射复合，从而降低外量子效率。

[0035] 另一个问题在于，非常薄的膜更经受诸如电极材料的侵入导致的短路的缺陷。以引用方式并入本文的美国专利 No. 6,333,458 描述了合并有一个或多个激子阻挡层的光敏异质结构，这解决了非常薄的膜 OPV 的一些问题。然而，需要其他解决方案来解决非常薄的膜的低光子吸收问题，无论膜是有机光导体还是无机光导体。

[0036] 在太阳能转换领域中常见的是使用被称为温斯顿（Winston）收集器的光学聚能器。这种聚能器已经被主要用于需要高热梯度的热太阳能收集装置中。在较小程度上，它们与光伏太阳能转换装置一起使用。然而，想到的是，这种应用涉及期望在光初始入射到有源光导体介质上时出现光子吸收的装置。如果使用非常薄的光导体层，则有可能被会聚的辐射中的许多将被吸收。它可以被反射回器件环境，被基板吸收或者如果基板是透明则只是穿过。因此，单独使用聚能器没有解决薄光导电层的低光子吸收率问题。用于辐射监测的光聚能器还已经用于利用光电倍增（PM）管检测切伦科夫（Cerenkov）或其它辐射。PM 管以与诸如本发明的 OPV 的固态检测器完全不同的原理，即光电效应操作。在 PM 管中，光子吸收介质，即金属电极中的低光子吸收率不是问题，但与本文公开的 OPV 不同的是，PM 管需要高操作电压。

[0037] 光聚焦和光陷是提高薄膜光伏太阳能电池和光电检测器的性能的重要途径。然而，这种方案中通常使用的反射镜利用的是诸如银或金的金属，其可以导致由于反射镜的光谱吸收而造成入射光子的显著损失。因此，将有利的是，提供一种增加薄膜光伏太阳能电池或光电检测器中的光陷并且跨大光谱范围具有减少损失的结构。

[0038] 发明人近来已证实，借助外延生长之后从昂贵的母基板被剥离的薄的、高效 III-V 半导体太阳能电池的分子束外延（MBE）进行生长。这种过程与过去二十年中采用的传统 ELO 技术的明显不同在于，围绕“牺牲 ELO 层”生长“保护层”，牺牲 ELO 层通常被蚀刻掉以将有源器件外延（～ 2μm 厚）与母基板分开。在全文以引用方式并入本文的美国专利申请 No. 13/099,850 中描述了这个过程。通过使用复合保护层结构，消除了母晶片的化学和表面形态劣化，如图 1 中所示。

[0039] 因此，可以使经处理的晶片的表面比开始的晶片更平滑，并且其表面的化学性还是保持不变，因此不需要在为了生长附加的且最终也可去除的外延层而再使用之前进行晶片再抛光。因此，可以不确定地再使用母晶片，因为原始母晶片在此过程期间都没有被消耗或改变。事实上，只有包括薄膜、单晶、高效的太阳能电池有源区的外延有源层被从整个晶片表面去除，随后被冷焊（不使用增加成本、重量并且有可能失败的粘合剂）至第二薄膜“主”基板。

[0040] 由于基板是工艺中使用的最贵的材料，因此多次再使用的策略去除了作为材料成本的晶片，并且将其获得转换成了开支成本，从而基本上改变了基于单晶 III-V 的太阳能电池的成本结构。如果不使用粘合剂的情况下将太阳能电池的非常薄的有源外延层结合到金属或金属化塑料箔，则所得模块的重量和形式因子还受到有利影响。

发明内容

[0041] 为了努力解决上述需要中的至少一些，公开了一种超高效单结和多结薄膜太阳能电池。本公开还涉及无损伤外延剥离（ELO）工艺，其对于基板采用无粘合剂、可靠和质轻的冷焊结合，诸如对成形为复合抛物线金属箔聚能器的塑料或金属箔的结合。发明人已经发

现，将低成本天阳能电池制造和被成形为集成收集器的箔基板上的会聚太阳能强度的薄膜太阳能电池的超高效率相结合可以不仅导致模块自身的低成本，而且因为在超过 6W/gm 的功率密度下用箔（包括低成本集成聚能器）上的超轻质电池取代重模块，导致基础结构的显著成本降低。

[0042] 在一个实施例中，本公开涉及一种薄膜太阳能电池，该薄膜太阳能电池包括：第一基板；金属接触，其结合到所述第一基板；有源光伏区，其结合到所述金属接触；一个或多个第一保护层；AlAs 层；一个或多个第二保护层；第二基板，其中，所述第二基板。

[0043] 在另一个实施例中，本公开涉及一种薄膜太阳能电池，该薄膜太阳能电池包括：第一基板；金属接触，其结合到所述第一基板；有源光伏区，其结合到所述金属接触；一个或多个第一保护层，其中，所述第一保护层中的至少一个包括从 InGaP、GaAs、InGaAs、InP 和 InAlP 中选择的至少一种化合物；AlAs 层；一个或多个第二保护层，其中，所述第二保护层中的至少一个包括从 InGaP、GaAs、InGaAs、InP 和 InAlP 中选择的至少一种化合物；第二基板，其中，所述第二基板包括从 GaAs 和 InP 中选择的至少一种化合物。

[0044] 在又一个实施例中，本公开涉及一种执行外延剥离工艺的方法，该方法包括：在第一基板上生长一个或多个第一保护层；生长 AlAs 层；生长一个或多个第二保护层；在所述第二保护层的顶部上沉积至少一个有源光伏电池层；用金属涂敷顶部的有源光伏电池层；用金属涂敷第二基板；将两个金属表面压到一起，以形成冷焊结合；用选择性化学蚀刻剂去除 AlAs 层。

[0045] 在另一个实施例中，本公开涉及一种执行外延剥离工艺的方法，该方法包括：在第一基板上生长一个或多个第一保护层，其中，所述保护层中的至少一个包括从 InGaP、GaAs、InGaAs、InP 和 InAlP 中选择的化合物；生长 AlAs 层；生长一个或多个第二保护层，其中，所述保护层中的至少一个包括从 InGaP、GaAs、InGaAs、InP 和 InAlP 中选择的化合物；在第二保护层的顶部上沉积至少一个有源光伏电池层；用金属涂敷顶部的有源光伏电池层；用金属涂敷第二基板；将两个金属表面压到一起，以形成冷焊结合；用选择性化学蚀刻剂去除 AlAs 层。

附图说明

[0046] 除了以上讨论的主题之外，本发明包括多个其它示例性特征，诸如下文中说明的示例性特征。要理解，以上描述和以下描述都只是示例性的。

[0047] 附图被合并并且构成本说明书的一部分。

[0048] 图 1 是示出针对基于 InP 的太阳能电池的根据本公开的 ELO 工艺的示意图。

[0049] 图 2 是两英寸的 InP 外延层被剥离并且结合到涂敷有 Au 的 Kaption 片材。ITO 接触件形成肖特基太阳能电池。

[0050] 图 3 是在使用保护层和不使用保护层的情况下，在第一 ELO 工艺和第二 ELO 工艺之后的原始开盒即用（epi-ready）InP 基板和被恢复表面的原子力显微图像。

[0051] 图 4 是表示电池参数的测试数据和代表性 GaAs PV 电池层结构。

[0052] 图 5 是示出 23.9% 效率的首次生长电池和在再使用的晶片上生长的 22.8% 效率的电池的四象限电流电压和外量子效率（插图）。

[0053] 图 6 是示出根据本公开的应用于 InP 材料的 ELO 工艺的示意图。

[0054] 图 7 是使用 AlAs 层和 AlAs 剥离层的三层保护方案的示意图。

[0055] 图 8 是根据本公开提出的多结电池结构的示意图。

[0056] 图 9 是（a）传统 N/P 隧道结和示出减小的隧穿势垒的（b）N/ErP/P 结的示意图。

[0057] 图 10 是冷焊结合的 ELO 多结电池的集成反射器的示意图。

具体实施方式

[0058] 在图 1 中示意性示出 ELO 工艺的一个实施例。先开始外延生长化学形式上不同的、由 InGaAs 和 Inp 组成的薄“保护层”、AlAs 的牺牲层、InP 和 InGaAs 的第二组保护层和最终的有源光伏电池层。接下来，顶部外延层被涂敷有 Au，作为非常薄的塑料（例如，Kapton™，由 DuPont 注册商标的聚酰亚胺膜）主基板。通过仅用几千帕的压力将这两个干净 Au 表面压到一起，它们在电子上形成连续、永久的、无粘合剂的冷焊结合，这种结合的性质与单个体的 Au 膜无差别。

[0059] 一旦结合到塑料柄部，晶片就为 ELO 做好准备。冷焊结合只用于 ELO 工艺（外延层在进行剥离从而剥脱母基板以备最终再使用之前永久地附着到箔基板），但还用作最终在上面制作太阳能电池的新主基板的粘合剂。

[0060] 用冷焊取代剥离中传统使用的粘合剂具有几点益处：（1）附着于箔基板变得简单并且是制作工序的一体化部分，（ii）它的重量轻，因为它完全去除了粘合剂层，（iii）它在热学上和电学上是“透明的”，因为冷焊界面与膜的主体是不可区分的，（iv）它是耐用的并且耐受故障。使用诸如 HF:H_2O，1:10 的选择性化学蚀刻剂去除 4nm 至 10nm 厚的 AlAs 牺牲 ELO 层，将整个晶片与光伏外延层分开，从而使保护层被暴露。最靠近 AlAs ELO 层（在这种情况下，InP）的保护层的目的在于提供 $>10^8$:1 的蚀刻选择性，并且通过突然止于 InGaAs 保护层表面的第二湿蚀刻（HCl:H_3PO_4，3:1）被从基板和分开的外延层两者去除。第二保护层的要求是，它可以通过突然止于 InP 基板的湿蚀刻剂被去除。使用 H_2SO_4:H_2O_2:H_2O（1:1:10）之后用 $C_6H_8O_7$:H_2O_2（20:1）从晶片去除 InGaAs 层，H_2SO_4:H_2O_2:H_2O（1:1:10）和 $C_6H_8O_7$:H_2O_2（20:1）对于 InP 基板、InP 缓冲层和外延层都具有高选择性，并且都有助于去除在上一个蚀刻之后保留下来的任何碎屑或凹凸不平。通过溅射氧化铟锡（ITO）肖特基接触，在附着于 Kapton™ 柄部的外延层上制作太阳能电池。在图 2 中示出在 1 倍太阳光强（1sun）AM1.5G 照射下效率为～15% 的所得的柔性 InP-TIO 肖特基太阳能电池。这些结合的外延片材已经重复循环至 >200℃，而没有层离。

[0061] 在后续生长之前，用溶剂清洁基板，经由曝光于 UV/O 区生长意图的氧化物，然后返回至生长腔室。已经对单个基板采用多次该处理，以验证 InP 晶片的无劣化再使用，并且如图 3 中所示，可以提高表面的光滑度，使其优于在允许无限再使用的原则下初始使用的商用开盒即用晶片的光滑度。

[0062] 发明人近期已经将这种无损伤再生长工艺扩展到在母晶片上制作的基于 GaAs 的单 p-n 结光伏电池，从而导致 23.9% 的效率。图 4 是这种电池的示意性表示。剥离工艺与用于 InP 电池的工艺类似，尽管用三层（InGaP/GaAs/InGaP）全晶格匹配（与 AlAs 牺牲层匹配）系统取代用于 InP 的两个保护层方案。这允许提高层之间的蚀刻选择性，同时去除在 ELO 工艺中遭致的碎屑或表面凹凸不平。在 HF 中去除 AlAs 层，之后分别用 HCl:H_3PO_4（1:1）和 H_3PO_4:H_2O_2:H_2O（3:1:25）去除 InGaP 和 GaAs 保护层。

[0063]　在这个工艺之后，在母晶片上生长第二电池，从而达到 22.8% 的效率。第一生长和第二生长之间的功率转换效率的略微（1%）减小是由于干台面绝缘蚀刻配方造成的，从而导致填充因子的略微减小（参见图 4）。此外，抗反射涂层厚度不是最佳的，从而减小了外量子效率和短路电流，如图 5 中所示。然而，当涂层厚度最佳时，期望的是甚至更高的效率，例如，大于 25% 的效率。

[0064]　在一个实施例中，可以使用基于全晶格匹配 InGaP/GaAs/InGaP 三层的保护层方案。这三层提供了蚀刻化学性，具有再生产地去除保护层并且暴露原始（物理和化学上未受损）表面所需的、层之间的充分比率选择性。在一个实施例中，再生长的薄膜电池经由冷焊结合到涂敷 Au 的塑料（Kapton™）基板。已经表明，对于第一生长晶片可以实现 PCE=23.9%，并且对于再使用晶片可以实现 PCE=22.8%，这超过了 20% 的下一代光伏 II 标准（参见图 5）。在图 6 中示出实际 ELO 工艺设备和方法的绘图。

[0065]　在各次再使用之后，可以彻底研究母晶片和被剥离的外延层二者的损伤或微小劣化。这些方法包括用于确定生长和再生长表面的化学变化的 X 射线光电子能谱仪（XPS）、原子力显微镜、扫描电子显微镜、用于确定表面形态变化的表面轮廓曲线仪、用于检验外延主体内遭致的缺陷的剖面透射电子显微镜、使用二次离子质谱学（SIMS）的组分深度分布。

[0066]　还可以使用标准照射条件（1 倍太阳光强，AM1.5G 光谱）对包括抗反射涂层的成品电池进行电学测试。将被测量的参数包括 PCE、填充因子（FF）、开路电压（V_{OC}）、短路电流（J_{SC}）、串联和并联电阻。

[0067]　已经发现，将含 Ga 化合物（即，GaAs，并且较小程度上，InGaP）延长暴露于 HF 导致难以去除的表面污染。然而，对于暴露于 HF 超过 7 天的 InP 表面不存在这种反应。在一个实施例中，位于 AlAs 牺牲层正下方的应变 InP 的薄层将提高表面的保真度，如图 7 中所示。

[0068]　InP 的厚度限于防止应变松弛，应变松弛会降低后续生长的 PV 层质量。GaAs 上的 InP 的临界厚度在 5 单层和 6 单层之间，对应于～ 1.7nm。在这种情况下，保护层方案将包括 InGaP/GaAs/InP 或 InGaP/GaAs/InGaP/InP，其中，后一结构中的附加 InGaP 层提供对 GaAs 的改进保护。

[0069]　在另一个实施例中，通过使用另外的材料组合，例如，通过取代与 InAlP 相邻的 InGaP 层，执行蚀刻选择性和保持原来购买的晶片质量。InAlP/InGaP/GaAs/InAlP 结构会是有利的，因为可以用突然止于 GaAs （>400:1 蚀刻率）的 $HCl:H_2O$ （1:5）蚀刻 InAlP，而用于蚀刻 InGaP 的 $HCl:H_3PO_4$ （1:1）缓慢地侵袭 GaAs，从而导致凹凸不平。通过取代与 AlAs 层相邻的 InAlP，InAlP 被 HF 侵袭并且减少氧化砷的集结，这样可以减缓剥离工艺。另外，InGaP 可以被用作 GaAs 蚀刻（$H_3PO_4:H_2O_2:H_2O$, 3:1:25）的蚀刻停止件，以确保在最终蚀刻步骤中去除下面的 InAlP 层。

[0070]　通过结合到诸如涂敷 Au 的 Cu 箔的金属箔基板，使用用于冷焊的低价格金属（例如，用 Ag 代替 Au）、减少的 HF 消耗、减小保护层厚度并且加速剥离过程，可以另外降低成本。延长暴露于用于溶解 AlAs 牺牲层的 HF 限制了对可以采用的金属主基板的选择。在一个实施例中，使用可以用于冷焊的铜箔增大了在暴露于 HF 时的抗性，因为它们的使用可以比用诸如 Au 的贵金属涂敷的箔简单。使用 Cu 箔的另外的益处是其高导热率（～ $4W\ cm^{-1}℃^{-1}$），可以利用该导热率从聚能电池中提取热。

[0071]　还公开了满足图 8 中示出的两个电池示例结构的非常高效的多结（GaAs/InGaP）

太阳能电池。

[0072] 设计相对于传统多结电池生长工序被颠倒，以适应无粘合剂冷焊工艺中使用的“颠倒”结合几何体；该结构包括 25%GaAs 电池构架。在这种情况下，GaAs 电池厚度减小至 2μm（基于传统基板的电池的 50%），因为反射性的全覆盖欧姆接触允许入射光两次穿过器件有源区。主要的焦点将是为了效率最大而优化串联 PV 结构，包括 InGaP 电池设计（层厚度，窗口层、层组分等），从而改进堆叠中元件之间的宽间隙隧道结（TJ），并且这个多结电池的大面积内完成多剥离工艺。

[0073] 将用 n 型材料在 p 型层的顶部上生长太阳能电池，而必须用相反极性生长隧道结。电池可以采用在所有或许多 p 型层中进行碳掺杂，因为碳不容易像传统 p 掺杂物 Be 一样迁移至生长表面。因为串联电池通常受 GaAs 电池中的电流限制，所以 InGaP 电池厚度需要被调节成与 InGaP 电池和 GaAs 电池电流匹配；期望 InGaP 层的厚度在 0.55μm 至 0.80μm 的范围内。

[0074] 对于高性能串联电池，有效隧道结（TJ）是必要的。它们需要在电压和吸收方面都几乎无损失。有利的是，在 MJ 电池中使用 InGaP TJ 以避免会高达 3% 的 GaAs TJ 吸收。传统 TJ 是突变 P+/N+ 结，其中，电子可以直接从 n 型侧的导带直接隧穿至 p 型侧的价带（图 9(a)）。对于 MBE 生长宽带隙 TJ 几乎没有执行工作，尽管使用 MBE 已经报道了高得足以传输在 1 倍太阳光强照射下产生的电流的掺杂水平。

[0075] 一个实施例涉及在 1 倍太阳光强下具有几十毫伏压降的 InGaP 隧结。研究表明，Be 和 Si 是合适的掺杂物（分别实现 $3.7\text{x}10^{19}$ 和 $1.8\text{x}10^{19}\text{cm}^{-3}$ 的密度）。然而，如果需要减小的隧穿电阻，诸如通过向 GaAs 隧结添加 ErAs，可以完成在 P+/N+ 界面处使用经设计的缺陷。在这种情况下，可以如图 9b 中所示使用 ErP 或 LuP。ErP 或 LuP 在半导体表面上形成外延岛，该外延岛是～ 4 单层厚，是金属，并且将隧穿过程分成两个步骤使隧穿可能性显著更高。通过在 TJ 中采用 ErP，会导致隧穿电流中的大小增加几个数量级，并且造成所制作的 PV 电池中预期电流的亚毫伏范围内的压降。

[0076] 如单结电池的情况中一样，可以在生长 ELO 再使用循环的每次重复之后，微观并且化学地检验多结电池。可以使用标准照明条件（AM1.5G 光谱）但是在高达 10 倍太阳光强的强度范围内电学地测试包括抗反射涂层的成品电池。将被测量的参数包括 PCE、填充因子、开路电压、短路电流、串联和并联电阻，如单结电池的情况中一样。

[0077] 结合到反射性和柔性基板的薄膜多结电池提供将太阳能收集器与薄膜电池集成而没有引入明显附加成本的独特机会。图 10 示出由 ELO 多结电池组成的带结合到较大的、柔性的反射膜的中心。然后，将膜模制（通过在导热或有源冷却预型件中放置）成复合抛物线收集器（例如，CPC、或温斯顿收集器）的形状。这种几何体将平行的阳光光线会聚到其焦点处的电池带，并且将漫射光收集到接受光锥内。

[0078] 圆柱形温斯顿型收集器中通常使用的小会聚水平（4-10X）允许会聚器高度有效，并且引导显著量将光漫射到电池中。通过 $\text{CEff}={}_{\text{CPC}}$ 给出收集效率，其中，${}_{\text{CPC}}$ 是 CPC 的有效透射率，包括公共反射器材料的～ 2% 的多次反射损失。漫射光的校正是 =1- (1-1/C)Gdiff/Gdir，其中，C 是意图会聚度，Gdiff/Gdir 是漫射光与总入射光的比率。通常，对于少云天，Gdiff/Gdir 是～ 0.11。然后，对于 C=4，AM1.5G 下 =90%，这与 AM1.5D 下可用的功率相当。

[0079] 对于 4X CPC，并且假设太阳能电池带宽度是 1cm，然后孔是 4cm 宽 ×10cm 深，从而

提供与单个家庭居所中使用的面板相兼容的实际形式因子。在较高会聚度下，聚能器的尺寸增大相当多。例如，相同 1cm 宽的电池带使用的 10X 会聚度需要 10cm 且深度～ 55cm 的孔。这可以减小至～ 40cm，并且对会聚效率的作用可忽略不计。[25] 所需要的反射材料的量对于 4X 会聚度是 4 至 5 倍大并且对于 10X 会聚度是 8 至 11 倍大。

[0080]　所使用的小会聚度的附加益处包括允许使用单轴追踪（按天或按季节，取决于收集器的方位），并且需要的无源冷却与较高会聚度需要的无源冷却相比简化。事实上，所使用的非常薄的基板大大简化了热传递：计算表明，抵靠无源冷却的 Cu 散热器放置的 10X 会聚度且 25mm 厚的 Kapton™ 基板只造成温度上升 5-20℃，从而不需要更具攻击性的冷却方法。

[0081]　注意的是，ELO 电池技术还可以应用于具有大会聚因子的系统；然而，这里，本公开只关注造成可应用于居住系统的简单且经济的设计的较小会聚度。期望这种集成的太阳能收集器 +ELO 多结聚能器电池组件的成本降低会完全降低会聚系统以及它们封装（归因于高 PCE）的成本。

[0082]　除非另外指明，否则说明书和权利要求书中使用的表示成分、反应条件等的所有数字将被理解为在所有情形下被术语“大约”修饰。因此，除非相反地指明，否则下面的说明书和所附的权利要求书中阐述的数字参数是可以取决于本发明企图得到的所需性质而变化的近似值。

[0083]　通过考虑本文公开的本发明的说明书和实践，本领域的技术人员将清楚本发明的其它实施例。说明书和实例旨在只被视为是示例性的，本发明的真实范围由随后的权利要求书指示。

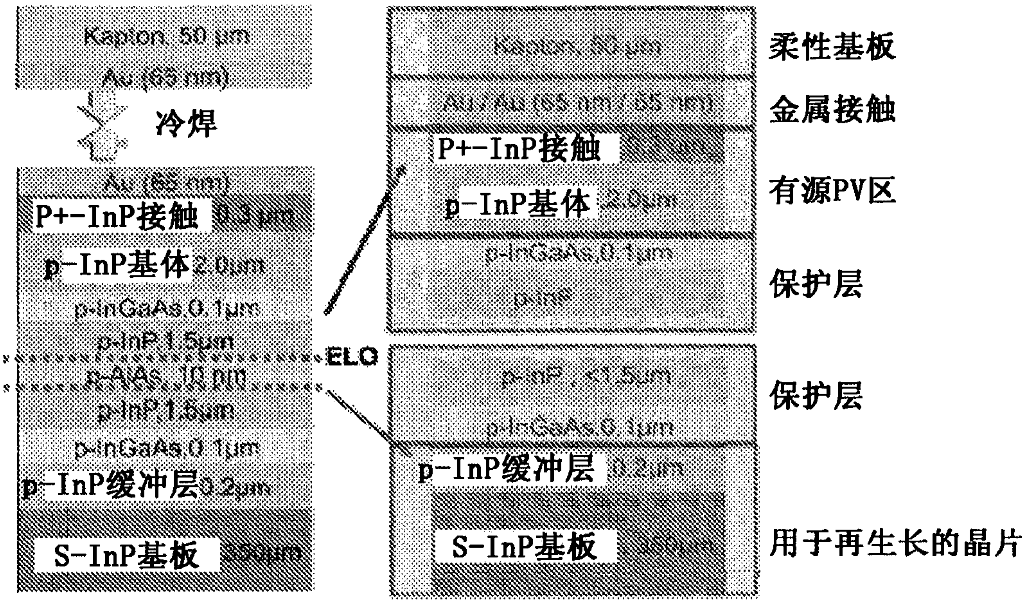
Kapton, 50 μm
Au (65 nm)
冷焊
Au (65 nm)
P+-InP接触 0.3 μm
p-InP基体 2.0μm
p-InGaAs,0.1μm
p-InP,1.5μm
ELO
p-AlAs, 10 nm
p-InP,1.5μm
p-InGaAs,0.1μm
p-InP缓冲层 0.2μm
S-InP基板 350μm
Kapton, 50 μm
柔性基板
Au / Au (65 nm / 65 nm)
金属接触
P+-InP接触 0.3 μm
p-InP基体 2.0μm
有源PV区
p-InGaAs,0.1μm
p-InP
保护层
p-InP, <1.5μm
p-InGaAs,0.1μm
保护层
p-InP缓冲层 0.2μm
S-InP基板 350μm
用于再生长的晶片

图 1

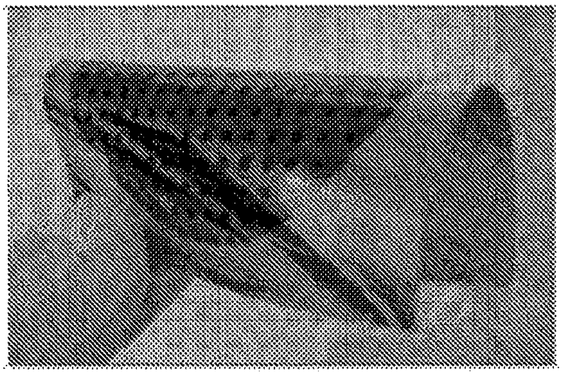

图 2

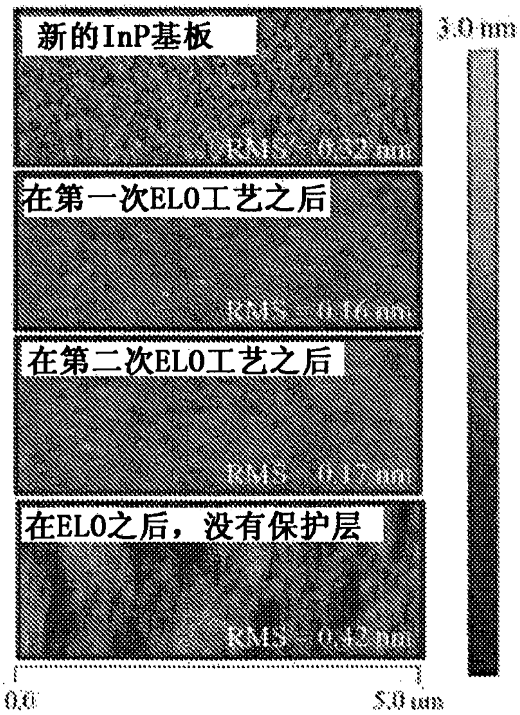
新的InP基板
RMS = 0.52 nm
在第一次ELO工艺之后
RMS = 0.46 nm
在第二次ELO工艺之后
RMS = 0.47 nm
在ELO之后，没有保护层
RMS = 0.42 nm
3.0 nm
0.0
5.0 μm

图 3

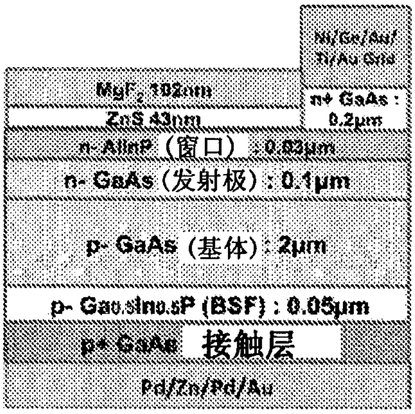

	Jsc[mA-cm²]	Voc [V]	FF	ηP
新的	28.2	1.01	84.4%	23.9%
再使用的	27.7	1.01	81.6%	22.8%

图 4

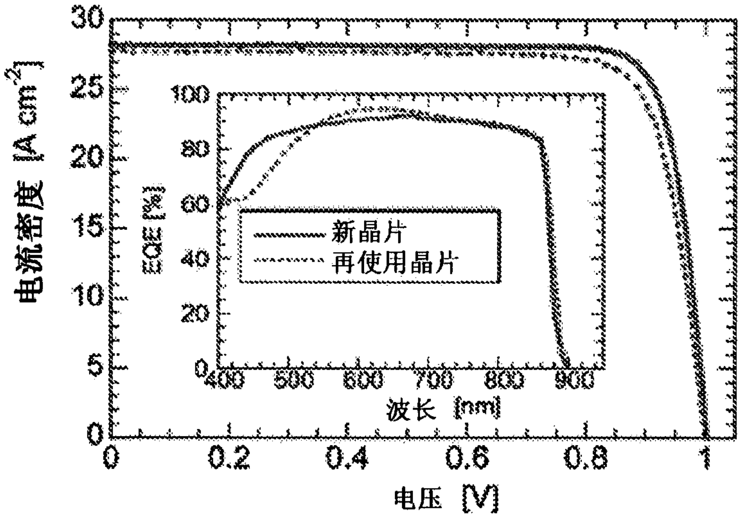

图 5

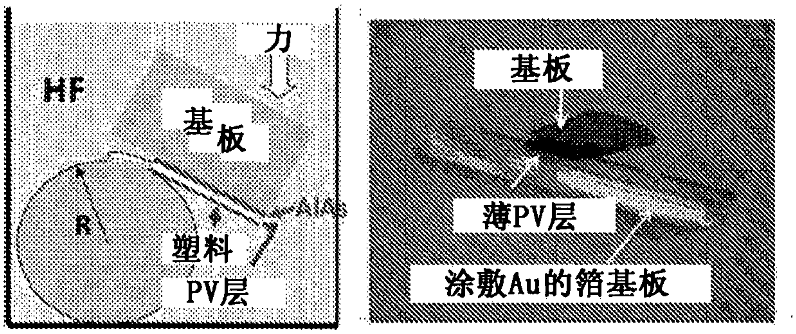
力
HF
基板
R
塑料
AlAs
PV层
基板
薄PV层
涂敷Au的箔基板

图 6


GaAs外延层
InGaP
GaAs
InGaP
AlAs剥离
InP
InGaP
GaAs
InGaP
GaAs基板

图 7

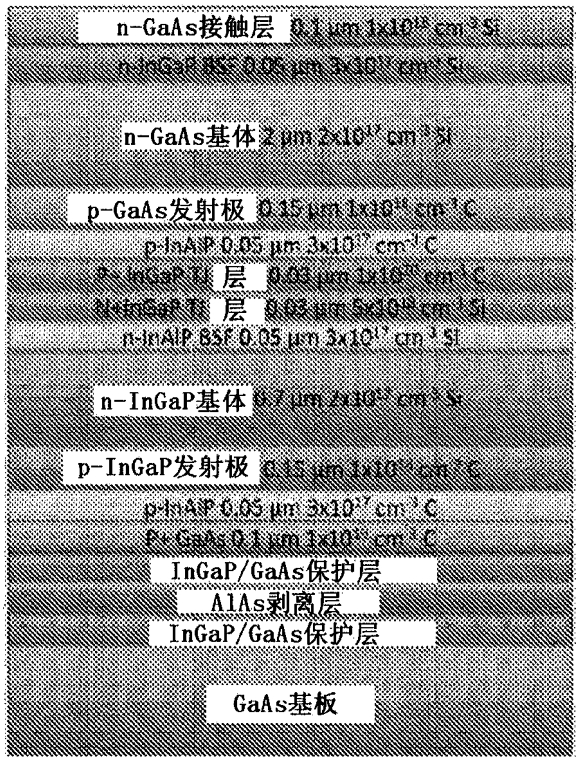
n-GaAs接触层 0.1 μm 1x10^{18} cm^{-3} Si
n-InGaP BSF 0.05 μm 3x10^{17} cm^{-3} Si
n-GaAs基体 2 μm 2x10^{17} cm^{-3} Si
p-GaAs发射极 0.15 μm 1x10^{18} cm^{-3} C
p-InAlP 0.05 μm 3x10^{17} cm^{-3} C
P+ InGaP TJ 层 0.03 μm 1x10^{20} cm^{-3} C
N+InGaP TJ 层 0.03 μm 5x10^{19} cm^{-3} Si
n-InAlP BSF 0.05 μm 3x10^{17} cm^{-3} Si
n-InGaP基体 0.7 μm 2x10^{17} cm^{-3} Si
p-InGaP发射极 0.15 μm 1x10^{18} cm^{-3} C
p-InAlP 0.05 μm 3x10^{17} cm^{-3} C
P+ GaAs 0.1 μm 1x10^{19} cm^{-3} C
InGaP/GaAs保护层
AlAs剥离层
InGaP/GaAs保护层
GaAs基板

图 8

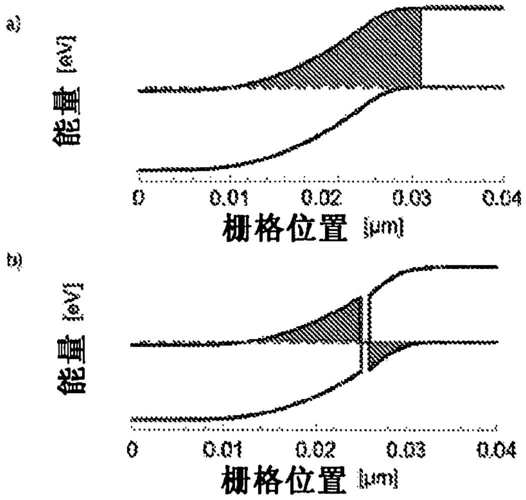
a)
能量 [eV]
0
0.01
0.02
0.03
0.04
栅格位置 [μm]
b)
能量 [eV]
0
0.01
0.02
0.03
0.04
栅格位置 [μm]

图 9

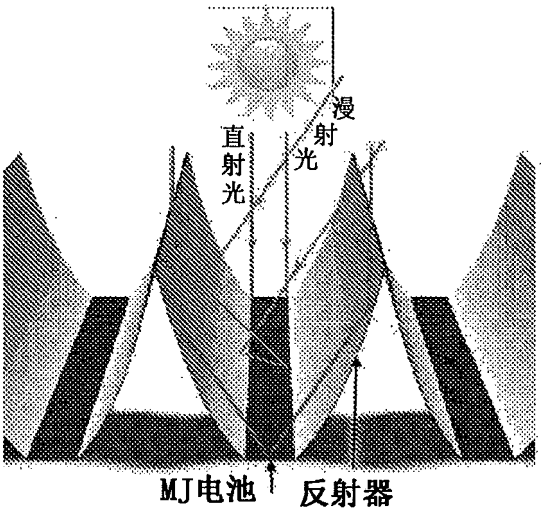
漫
射
光
直
射
光
MJ电池
反射器

图 10